

---

PART VI

---

High-Level Vision: Probabilistic and  
Inferential Methods



## 22

*Finding Templates  
Using Classifiers*

There are a number of important object recognition problems that involve looking for image windows that have a simple shape and stylized content. For example, frontal faces appear as oval windows, and (at a coarse scale) all faces look pretty much the same—a dark horizontal bar at the eyes and mouth, a light vertical bar along the nose, and not much texture on the cheeks and forehead. As another example, a camera mounted on the front of a car always sees relevant stop signs as having about the same shape and appearance.

This suggests a view of object recognition where we take all image windows of a particular shape and test them to tell whether the relevant object is present. If we don't know how big the object will be, we can search over scale, too; if we don't know its orientation, we might search over orientation as well; and so on. Generally, this approach is referred to as *template matching*. There are some objects that can be found effectively with a template matcher. Faces and road signs are important examples. Second, although many objects are hard to find with simple template matchers (it would be hard to find a person this way because the collection of possible image windows that represent a person is immense), there is some evidence that reasoning about *relations* among many different kinds of templates can be an effective way to find objects. In chapter 23, we explore this line of reasoning further.

The main issue to study in template matching is how one builds a test that can tell whether an oval represents a face. Ideally, this test is obtained using a large set of examples. The test is known as a *classifier*—a classifier is anything that takes a feature set as an input and produces a class label. In this chapter, we describe a variety of techniques for building classifiers, with examples of their use in vision applications. We first present the key ideas and terminology used (Section 22.1); we then show two successful classifiers built using histograms (Section 22.2); for more complex classifiers, we need to choose the features a classifier should use; and we discuss two methods in (Section 22.3). Finally, we describe two different methods for building classifiers

with current applications in vision. Section 22.4 is an introduction to the use of neural nets in classification, and Section 22.5 describes a useful classifier known as a support vector machine.

## 22.1 CLASSIFIERS

Classifiers are built by taking a set of labeled examples and using them to come up with a rule that assigns a label to any new example. In the general problem, we have a training dataset  $(\mathbf{x}_i, y_i)$ ; each of the  $\mathbf{x}_i$  consists of measurements of the properties of different types of object, and the  $y_i$  are labels giving the type of the object that generated the example. We know the relative costs of mislabeling each class and must come up with a rule that can take any plausible  $\mathbf{x}$  and assign a class to it.

The cost of an error significantly affects the decision that is made. In Section 22.1.1, we study this question. It emerges that the probability of a class label given a measurement is the key matter. In Section 22.1.2, we discuss methods for building appropriate models in a general way. Finally, we discuss how to estimate the performance of a given classifier (Section 22.1.5).

### 22.1.1 Using Loss to Determine Decisions

The choice of classification rule must depend on the cost of making a mistake. For example, doctors engage in classification all the time—given a patient, they produce the name of a disease. A doctor who decided that a patient suffering from a dangerous and easily treated disease is well is going to have problems. It would be better to err on the side of misclassifying healthy patients as sick even if doing so involves treating some healthy patients unnecessarily.

The cost depends on what is misclassified to what. Generally, we write outcomes as  $(i \rightarrow j)$ , meaning that an item of type  $i$  is classified as an item of type  $j$ . Each outcome has its own cost, which is known as a *loss*. Hence, we have a loss function that we write as  $L(i \rightarrow j)$ , meaning the loss incurred when an object of type  $i$  is classified as having type  $j$ . Since losses associated with correct classification should not affect the design of the classifier,  $L(i \rightarrow i)$  must be zero, but the other losses could be any positive numbers.

The *risk function* of a particular classification strategy is the expected loss when using it, as a function of the kind of item. The *total risk* is the total expected loss when using the classifier. Thus, if there were two classes, the total risk of using strategy  $s$  would be

$$R(s) = Pr\{1 \rightarrow 2 \mid \text{using } s\} L(1 \rightarrow 2) + Pr\{2 \rightarrow 1 \mid \text{using } s\} L(2 \rightarrow 1).$$

The desirable strategy is one that minimizes this total risk.

**Building a Two-Class Classifier That Minimizes Total Risk** Assume that the classifier can choose between two classes and we have a known loss function. There is some boundary in the feature space, which we call the *decision boundary*, such that points on one side belong to class one and points on the other side to class two.

We can resort to a trick to determine where the decision boundary is. It must be the case that, *for points on the decision boundary of the optimal classifier*, either choice of class has the same expected loss—if this weren't so, we could obtain a better classifier by always choosing one class (and so moving the boundary). This means that, for measurements on the decision boundary, choosing class one yields the same expected loss as choosing class two.

A choice of class one for a point  $\mathbf{x}$  at the decision boundary yields an expected loss

$$\begin{aligned} P\{\text{class is 2} \mid \mathbf{x}\} L(2 \rightarrow 1) + P\{\text{class is 1} \mid \mathbf{x}\} L(1 \rightarrow 1) &= P\{\text{class is 2} \mid \mathbf{x}\} L(2 \rightarrow 1) + 0 \\ &= p(2 \mid \mathbf{x})L(2 \rightarrow 1). \end{aligned}$$



You should watch the one's and two's closely here. Similarly, a choice of class two for this point yields an expected loss

$$P\{\text{class is 1} \mid \mathbf{x}\}L(1 \rightarrow 2) = p(1 \mid \mathbf{x})L(1 \rightarrow 2),$$

and these two terms must be equal. This means our decision boundary consists of the points  $\mathbf{x}$ , where

$$p(1 \mid \mathbf{x})L(1 \rightarrow 2) = p(2 \mid \mathbf{x})L(2 \rightarrow 1).$$

We can come up with an expression that is often slightly more practical by using Bayes' rule. Rewrite our expression as

$$\frac{p(\mathbf{x} \mid 1)p(1)}{p(\mathbf{x})}L(1 \rightarrow 2) = \frac{p(\mathbf{x} \mid 2)p(2)}{p(\mathbf{x})}L(2 \rightarrow 1)$$

and clear denominators to get

$$p(\mathbf{x} \mid 1)p(1)L(1 \rightarrow 2) = p(\mathbf{x} \mid 2)p(2)L(2 \rightarrow 1).$$

This expression identifies points  $\mathbf{x}$  on a class boundary; we now need to know how to classify points off a boundary.

At points off the boundary, we must choose the class with the *lowest* expected loss. Recall that if we choose class two for a point  $\mathbf{x}$ , the expected loss is

$$p(1 \mid \mathbf{x})L(1 \rightarrow 2),$$

etc. This means that we should choose class one if

$$p(1 \mid \mathbf{x})L(1 \rightarrow 2) > p(2 \mid \mathbf{x})L(2 \rightarrow 1)$$

and class two if

$$p(1 \mid \mathbf{x})L(1 \rightarrow 2) < p(2 \mid \mathbf{x})L(2 \rightarrow 1).$$

**A Classifier for Multiple Classes** From now on, we assume that  $L(i \rightarrow j)$  is zero for  $i = j$  and one otherwise – that is, that each outcome has the same loss. In some problems, there is another option, which is to refuse to decide which class an object belongs to. This option involves some loss, too, which we assume to be  $d < 1$  (if the loss involved in refusing to decide is greater than the loss involved in any decision, then we'd never refuse to decide).

For our loss function, the best strategy, known as the *Bayes classifier*, is given in Algorithm 22.1. The total risk associated with this rule is known as the *Bayes risk*; this is the smallest possible risk that we can have in using a classifier. It is usually rather difficult to know what the Bayes classifier—and hence the Bayes risk—is because the probabilities involved are not known exactly. In a few cases, it is possible to write the rule out explicitly. One way to tell the effectiveness of a technique for building classifiers is to study the behavior of the risk as the number of examples increases (e.g., one might want the risk to converge to the Bayes risk in probability if the number of examples is large). The Bayes risk is seldom zero as Figure 22.1 illustrates.

### 22.1.2 Overview: Methods for Building Classifiers

Usually, we do not know  $Pr\{\mathbf{x} \mid k\}$  exactly—which are often called *class-conditional densities*—or  $Pr\{k\}$ , and we must determine a classifier from an example dataset. There are two rather general strategies:

**Algorithm 22.1:** The Bayes classifier classifies points using the posterior probability that an object belongs to a class, the loss function, and the prospect of refusing to decide.

For a loss function

$$L(i \rightarrow j) = \begin{cases} 1 & i \neq j \\ 0 & i = j \\ d < 1 & \text{no decision} \end{cases}$$

the best strategy is

- if  $Pr\{k | \mathbf{x}\} > Pr\{i | \mathbf{x}\}$  for all  $i$  not equal to  $k$ , and if this probability is greater than  $1 - d$ , choose type  $k$
- if there are several classes  $k_1 \dots k_j$  for which  $Pr\{k_1 | \mathbf{x}\} = Pr\{k_2 | \mathbf{x}\} = \dots = Pr\{k_j | \mathbf{x}\} > Pr\{i | \mathbf{x}\}$  for all  $i$  not in  $k_1, \dots, k_j$ , choose uniformly and at random between  $k_1, \dots, k_j$
- if for all  $k$  we have  $Pr\{k | \mathbf{x}\} > Pr\{i | \mathbf{x}\} \leq 1 - d$ , refuse to decide.

- **Explicit probability models:** We can use the example data set to build a probability model (of either the likelihood or the posterior, depending on taste). There is a wide variety of ways of doing this, some of which we see in the following sections. In the simplest case, we know that the class-conditional densities come from some known parametric form of distribution. In this case, we can compute estimates of the parameters from the dataset and plug these estimates into the Bayes rule. This strategy is often known as a *plug-in classifier* (Section 22.1.3). This approach covers other parametric density models and other methods of estimating parameters. One subtlety is that the best estimate of a parameter may not give the best classifier because the parametric model may not

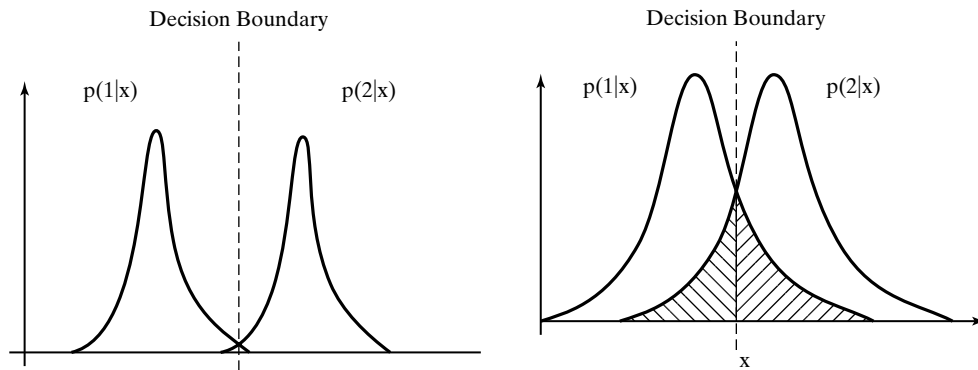


**Figure 22.1** This figure shows typical elements of a two-class classification problem. We have plotted  $p(\text{class}|x)$  as a function of the feature  $x$ . Assuming that  $L(1 \rightarrow 2) = L(2 \rightarrow 1)$ , we have marked the classifier boundaries. In this case, the Bayes risk is the sum of the amount of the posterior for class one in the class two region and the amount of the posterior for class two in the class one region (the hatched area in the figures). For the case on the left, the classes are well separated, which means that the Bayes risk is small; for the case on the right, the Bayes risk is rather large.

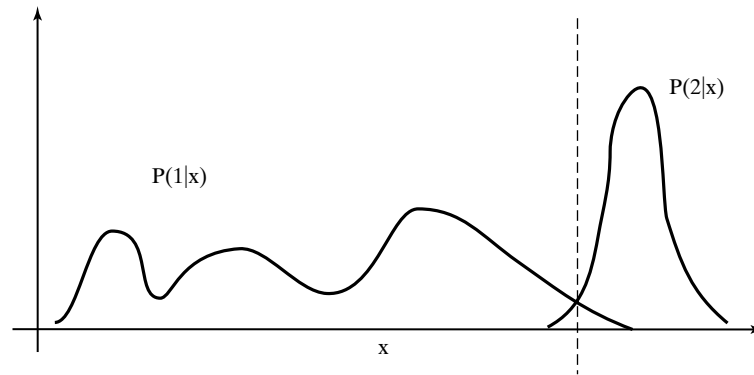


**Figure 22.2** The figure shows posterior densities for two classes. The optimal decision boundary is shown as a dashed line. Notice that, although a normal density may provide rather a poor fit to the posteriors, the quality of the classifier it provides depends only on how well it predicts the position of the boundaries. In this case, assuming that the posteriors are normal may provide a fairly good classifier because  $P(2|x)$  looks normal, and the mean and covariance of  $P(1|x)$  look as if they would predict the boundary in the right place.

be correct. Another subtlety is that a good classifier may be obtained using a parametric density model that is not an accurate description of the data (see Figure 22.2). In many cases, it is hard to obtain a satisfactory model with a small number of parameters. More sophisticated modeling tools (such as neural nets, which we deal with in some detail in Section 22.4) provides flexible density models that can be fitted using data.

- **Determining decision boundaries directly:** Quite bad probability models can produce good classifiers, as Figure 22.2 indicates. This is because the decision boundaries are what determine the performance of a classifier, not the details of the probability model (the main role of the probability model in the Bayes classifier is to identify the decision boundaries). This suggests that we might ignore the probability model and attempt to construct good decision boundaries directly. This approach is often extremely successful; it is particularly attractive when there is no reasonable prospect of modeling the data source. One strategy assumes that the decision boundary comes from one or another class and constructs an extremization problem to choose the best element of that class. A particularly important case comes when the data is *linearly separable*—which means that there exists a hyperplane with all the positive points on one side and all the negative points on the other—and thus that a hyperplane is all that is needed to separate the data (Section 22.5).

### 22.1.3 Example: A Plug-in Classifier for Normal Class-conditional Densities

An important plug-in classifier occurs when the class-conditional densities are known to be normal. We can either assume that the priors are known or estimate the priors by counting the number of data items from each class. Now we need to provide the parameters for the class-conditional densities. We do this as an estimation problem using the data items to estimate the mean  $\mu_k$  and covariance  $\Sigma_k$  for each class. Now since  $\log a > \log b$  implies  $a > b$ , we can work with the logarithm of the posterior. This yields a classifier of the form in Algorithm 22.2.

The term  $\delta(\mathbf{x}; \mu_k, \Sigma_k)$  in this algorithm is known as the *Mahalanobis distance* (e.g., see Ripley 1996). The algorithm can be interpreted geometrically as saying that the correct class

**Algorithm 22.2:** A plug-in classifier can be used to classify objects into classes if the class-conditional densities are known to be normal

Assume we have  $N$  classes, and the  $k$ th class contains  $N_k$  examples, of which the  $i$ th is written as  $\mathbf{x}_{k,i}$ .

For each class  $k$ , estimate the mean and standard deviation for that class-conditional density.

$$\boldsymbol{\mu}_k = \frac{1}{N_k} \sum_{i=1}^{N_k} \mathbf{x}_{k,i}; \quad \boldsymbol{\Sigma}_k = \frac{1}{N_k - 1} \sum_{i=1}^{N_k} (\mathbf{x}_{k,i} - \boldsymbol{\mu}_k)(\mathbf{x}_{k,i} - \boldsymbol{\mu}_k)^T;$$

To classify an example  $\mathbf{x}$ ,

Choose the class  $k$  with the smallest value of  $\delta(\mathbf{x}; \boldsymbol{\mu}_k, \boldsymbol{\Sigma}_k)^2 - Pr\{k\}$

where

$$\delta(\mathbf{x}; \boldsymbol{\mu}_k, \boldsymbol{\Sigma}_k) = \frac{1}{2} \left( (\mathbf{x} - \boldsymbol{\mu}_k)^T \boldsymbol{\Sigma}_k^{-1} (\mathbf{x} - \boldsymbol{\mu}_k) \right)^{(1/2)}.$$

is the one whose mean is closest to the data item *taking into account the variance*. In particular, distance from a mean along a direction where there is little variance has a large weight and distance from the mean along a direction where there is a large variance has little weight. This classifier can be simplified by assuming that each class has the same covariance (with the advantage that we have fewer parameters to estimate). In this case, because the term  $\mathbf{x}^T \boldsymbol{\Sigma}^{-1} \mathbf{x}$  is common to all expressions, the classifier actually involves comparing expressions that are *linear in  $\mathbf{x}$*  (see Exercises). If there are only two classes, the process boils down to determining whether a linear expression in  $\mathbf{x}$  is greater than or less than zero (Exercises).

#### 22.1.4 Example: A Nonparametric Classifier Using Nearest Neighbors

It is reasonable to assume that example points near an unclassified point should indicate the class of that point. *Nearest neighbors* methods build classifiers using this heuristic. We could classify a point by using the class of the nearest example whose class is known, or use several example points and make them vote. It is reasonable to require that some minimum number of points vote for the class we choose.

A  $(k, l)$  nearest neighbor classifier finds the  $k$  example points closest to the point being considered, and classifies this point with the class that has the highest number of votes, as long as this class has more than  $l$  votes (otherwise the point is classified as unknown). A  $(k, 0)$ -nearest neighbor classifier is usually known as a *k-nearest neighbor classifier*, and a  $(1, 0)$ -nearest neighbor classifier is usually known as a *nearest neighbor classifier*.

Nearest neighbor classifiers are known to be good, in the sense that the risk of using a nearest neighbor classifier with a sufficiently large number of examples lies within quite good bounds of the Bayes risk. As  $k$  grows, the difference between the Bayes risk and the risk of using a  $k$ -nearest neighbor classifier goes down as  $1/\sqrt{k}$ . In practice, one seldom uses more than three nearest neighbors. Furthermore, if the Bayes risk is zero, the expected risk of using a  $k$ -nearest neighbor classifier is also zero (see Devroye, Györfi & Lugosi 1996 for more detail on all these points).

Nearest neighbor classifiers come with some computational subtleties, however. The first is the question of finding the  $k$  nearest points, which is no mean task in a high-dimensional

space (surprisingly, checking the distance to each separate example one by one is, at present, a competitive algorithm). This task can be simplified by noticing that some of the example points may be superfluous. If, when we remove a point from the example set, the set still classifies every point in the space in the same way (the decision boundaries have not moved), that point is redundant and can be removed. However, it is hard to know *which* points to remove. The decision regions for  $(k, l)$ -nearest neighbor classifiers are convex polytopes; this makes familiar algorithms available in 2D (where Voronoi diagrams implement the nearest neighbor classifier) but leads to complications in high dimensions.

**Algorithm 22.3:** A  $(k, l)$  nearest neighbor classifier uses the type of the nearest training examples to classify a feature vector

Given an feature vector  $\mathbf{x}$

1. determine the  $k$  training examples that are nearest,  $\mathbf{x}_1, \dots, \mathbf{x}_k$ ;
2. determine the class  $c$  that has the largest number of representatives  $n$  in this set;
3. if  $n > l$ , classify  $\mathbf{x}$  as  $c$ , otherwise refuse to classify it.

A second difficulty in building such classifiers is the choice of distance. For features that are obviously of the same type, such as lengths, the usual metric may be good enough. But what if one feature is a length, one is a color, and one is an angle? One possibility is to use a covariance estimate to compute a Mahalanobis-like distance.

### 22.1.5 Estimating and Improving Performance

Typically, classifiers are chosen to work well on the training set, and this can mean that the performance of the classifier on the training set is a poor guide to its overall performance. One example of this problem is the (silly) classifier that takes any data point and, if it is the same as a point in the training set, emits the class of that point and otherwise chooses randomly between the classes. This classifier has been learned from data, and has a zero error rate on the training dataset; it is likely to be unhelpful on any other dataset, however.

The difficulty occurs because classifiers are subject to *overfitting* effects. The phenomenon, which is known by a variety of names (*selection bias* is quite widely used), has to do with the fact that the classifier is chosen to perform well *on the training dataset*. The training data is a (possibly representative) subset of the available possibilities. The term *overfitting* is descriptive of the source of the problem, which is that the classifier's performance on the training dataset may have to do with quirks of that dataset that don't occur in other sets of examples. If the classifier does this, it is quite possible that it will perform well on the training data and badly on any other dataset (this phenomenon is often referred to as *generalizing badly*).

Generally, we expect classifiers to perform somewhat better on the training set than on the test set (e.g., see Figure 22.18, which shows training set and test set errors for a classifier that is known to work well). Overfitting can result in a substantial difference between performance on the training set and performance on the test set. This leaves us with the problem of predicting performance. There are two possible approaches: We can hold back some training data to check the performance of the classifier (an approach we describe later), or we can use theoretical methods to bound the future error rate of the classifier (see, e.g., Vapnik 1996 or 1998).

**Estimating Total Risk with Cross-Validation** We can make direct estimates of the expected risk of using a classifier if we split the dataset into two subsets, train the classifier on

one subset, and test it on the other. This is a waste of data, particularly if we have few data items for a particular class, and may lead to an inferior classifier. However, if the size of the test subset is small, the difficulty may not be significant. In particular, we could then estimate total risk by averaging over all possible splits. This technique, known as *cross-validation* allows an estimate of the likely future performance of a classifier, at the expense of substantial computation.

**Algorithm 22.4:** Cross-Validation

Choose some class of subsets of the training set, for example, singletons.

For each element of that class, construct a classifier by omitting that element in training, and compute the classification errors (or risk) on the omitted subset.

Average these errors over the class of subsets to estimate the risk of using the classifier trained on the entire training dataset.

The most usual form of this algorithm involves omitting single items from the dataset and is known as *leave-one-out cross-validation*. Errors are usually estimated by simply averaging over the class, but more sophisticated estimates are available (see, e.g., Ripley 1996). We do not justify this tool mathematically; however, it is worth noticing that leave-one-out cross-validation, in some sense, looks at the sensitivity of the classifier to a small change in the training set. If a classifier performs well under this test, then large subsets of the dataset look similar to one another, which suggests that a representation of the relevant probabilities derived from the dataset might be quite good.

**Using Bootstrapping to Improve Performance** Generally, more training data leads to a better classifier. However, training classifiers with large datasets can be difficult, and there are diminishing returns. Typically, only a relatively small number of example items are really important in determining the behavior of a classifier (we see this phenomenon in greater detail in Section 22.5). The really important examples tend to be rare cases that are quite hard to discriminate. This is because these cases affect the position of the decision boundary most significantly. We need a large dataset to ensure that these cases are present, but it appears inefficient to go to great effort to train on a large dataset, most of whose elements aren't particularly important.

There is a useful trick that avoids much redundant work. We train on a subset of the examples, run the resulting classifier on the rest of the examples, and then insert the false positives and false negatives into the training set to retrain the classifier. This is because the false positives and false negatives are the cases that give the most information about errors in the configuration of the decision boundaries. This strategy is known as *bootstrapping* (the name is potentially confusing because there is an unrelated statistical procedure known as bootstrapping; nonetheless, we're stuck with it at this point).

## 22.2 BUILDING CLASSIFIERS FROM CLASS HISTOGRAMS

One simple way to build a probability model for a classifier is to use a histogram. If a histogram is divided by the total number of pixels, we get a representation of the class-conditional probability density function. It is a fact that, as the dataset gets larger and the histogram bins

get smaller, the histogram divided by the total number of data items will almost certainly converge to the probability density function (e.g., Devroye, Györfi & Lugosi 1996, Vapnik 1996, and 1998). In low-dimensional problems, this approach can work quite well (Section 22.2.1). It isn't practical for high-dimensional data because the number of histogram bins required quickly becomes intractable unless we use strong independence assumptions to control the complexity (Section 22.2.2).

### 22.2.1 Finding Skin Pixels Using a Classifier

Skin finding is useful for activities like building gesture-based interfaces. Skin has a quite characteristic range of colors, suggesting that we can build a skin finder by classifying pixels on their color. Jones & Rehg (1999) construct a histogram of RGB values due to skin pixels and a second histogram of RGB values due to non-skin pixels. These histograms serve as models of the class-conditional densities.

We write  $\mathbf{x}$  for a vector containing the color values at a pixel. We subdivide this color space into boxes and count the percentage of skin pixels that fall into each box—this histogram supplies  $p(\mathbf{x} \mid \text{skin pixel})$ , which we can evaluate by determining the box corresponding to  $\mathbf{x}$  and then reporting the percentage of skin pixels in this box. Similarly, a count of the percentage of non skin pixels that fall into each box supplies  $p(\mathbf{x} \mid \text{not skin pixel})$ . We need  $p(\text{skin pixel})$  and  $p(\text{not skin pixel})$ —or rather, we need only one of the two as they sum to one. Assume for the moment that the prior is known. We can now build a classifier using Bayes' rule to obtain the posterior (keep in mind that  $p(\mathbf{x})$  is easily computed as  $p(\mathbf{x} \mid \text{skin pixel}) + p(\mathbf{x} \mid \text{not skin pixel})$ ).

One way to estimate the prior is to model  $p(\text{skin pixel})$  as the fraction of skin pixels in some (ideally large) training set. Notice that our classifier compares

$$\frac{p(\mathbf{x} \mid \text{skin})p(\text{skin})}{p(\mathbf{x})}L(\text{skin} \rightarrow \text{not skin})$$

with

$$\frac{p(\mathbf{x} \mid \text{not skin})p(\text{not skin})}{p(\mathbf{x})}L(\text{not skin} \rightarrow \text{skin}).$$

Now by rearranging terms and noticing that  $p(\text{skin} \mid \mathbf{x}) = 1 - p(\text{not skin} \mid \mathbf{x})$ , our classifier becomes

- if  $p(\text{skin} \mid \mathbf{x}) > \theta$ , classify as skin
- if  $p(\text{skin} \mid \mathbf{x}) < \theta$ , classify as not skin
- if  $p(\text{skin} \mid \mathbf{x}) = \theta$ , choose classes uniformly and at random

where  $\theta$  is an expression that doesn't depend on  $\mathbf{x}$  and encapsulates the relative loss. This yields a family of classifiers, one for each choice of  $\theta$ . For an appropriate choice of  $\theta$ , the classifier can be good (Figure 22.3).

Each classifier in this family has a different false-positive and false-negative rate. These rates are functions of  $\theta$ , so we can plot a parametric curve that captures the performance of the family of classifiers. This curve is known as a *receiver operating curve (ROC)*. Figure 22.4 shows the ROC for a skin finder built using this approach. The ROC is invariant to choice of prior (Exercises)—this means that if we change the value of  $p(\text{skin})$ , we can choose some new value of  $\theta$  to get a classifier with the same performance. This yields another approach to estimating a prior. We choose some value rather arbitrarily, plot the loss on the training set as a function of  $\theta$ , and then select the value of  $\theta$  that minimizes this loss.



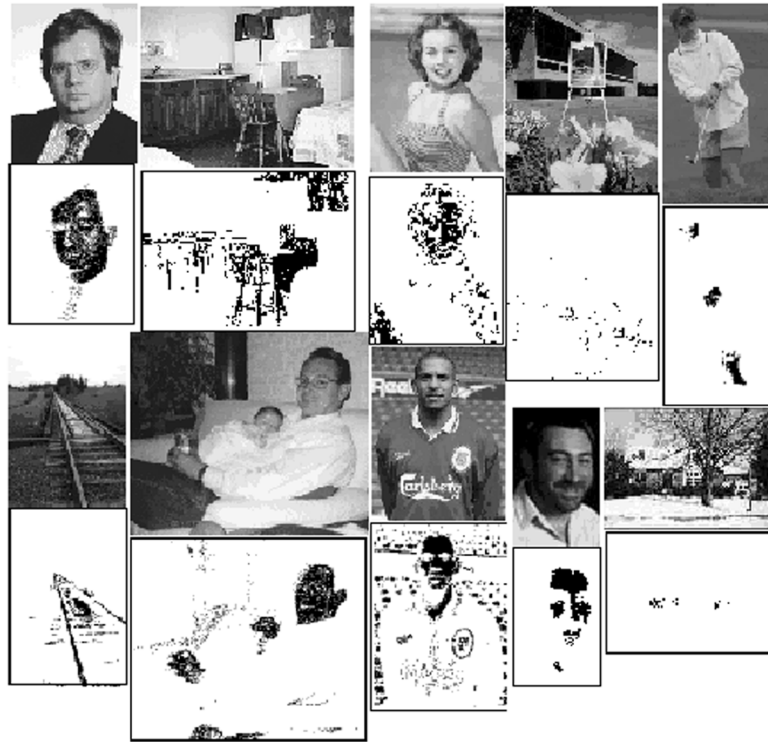


**Figure 22.3** The figure shows a variety of images together with the output of the skin detector of Jones and Rehg applied to the image. Pixels marked black are skin pixels and white are background. Notice that this process is relatively effective and could certainly be used to focus attention on, say, faces and hands. Reprinted from “Statistical color models with application to skin detection,” by M.J. Jones and J. Rehg, *Proc. Computer Vision and Pattern Recognition*, 1999 © 1999, IEEE

### 22.2.2 Face Finding Assuming Independent Template Responses

Histogram models become impractical in high dimensions because the number of boxes required goes up as a power of the dimension. We can dodge this phenomenon. Recall that independence assumptions reduce the number of parameters that must be learned in a probabilistic model (or see the chapter on probability on the book website); by assuming that terms are independent, we can reduce the dimension sufficiently to use histograms. Although this appears to be an aggressive oversimplification—it is known by the pejorative name of *naïve Bayes*—it can result in useful systems. In one such system, due to Schneiderman & Kanade (1998), this model is used to find faces. Assume that the face occurs at a fixed, known scale (we could search smoothed and resampled versions of the image to find larger faces) and occupies a region of known shape. In the case of frontal faces, this might be an oval or a square; for a lateral face, this might be some more complicated polygon. We now need to model the image pattern generated by the face. This is a likelihood model—we want a model giving  $P(\text{image pattern} \mid \text{face})$ . As usual, it is helpful to think in terms of generative models; the process by which a face gives rise to an image patch. The set of possible image patches is somewhat difficult to deal with because it is big, but we can



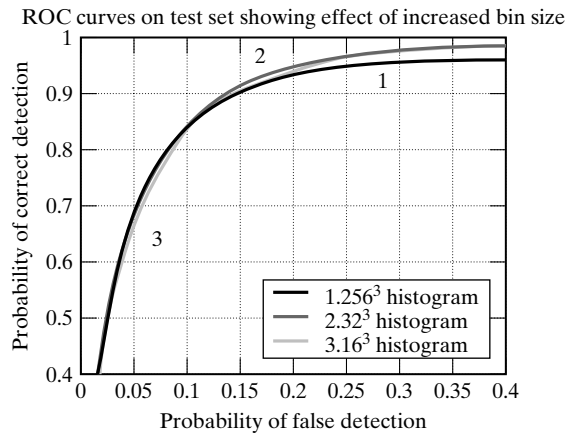


**Figure 22.4** The receiver operating curve for the skin detector of Jones and Rehg. This plots the detection rate against the false-negative rate for a variety of values of the parameter  $\theta$ . A perfect classifier has an ROC that, on these axes, is a horizontal line at 100% detection. Notice that the ROC varies slightly with the number of boxes in the histogram. *Reprinted from "Statistical color models with application to skin detection," by M.J. Jones and J. Rehg, Proc. Computer Vision and Pattern Recognition, 1999 © 1999, IEEE*

avoid this by dividing the image patch into a set of subregions and then labeling the subregions using a small set of labels.

An appropriate labeling can be obtained using a clustering algorithm and a large number of example images. For example, we might cluster the subregions in a large number of example images using  $k$ -means; now each cluster center represents a typical form of subregion. The subregions in our image patch can then be labeled with the cluster center to which they are closest. This approach has the advantage that minor variations in the image pattern—caused perhaps by noise, skin irregularities, and so on—are suppressed.

At this point, a number of models are available. The simplest practical model is to assume that the probability of encountering each pattern is independent of the configuration of the other patterns (but not of position) given that a face is present. This means that our model is

$$\begin{aligned} P(\text{image} \mid \text{face}) &= P(\text{label } 1 \text{ at } (x_1, y_1), \dots, \text{label } k \text{ at } (x_k, y_k) \mid \text{face}) \\ &= P(\text{label } 1 \text{ at } (x_1, y_1) \mid \text{face}) \dots P(\text{label } k \text{ at } (x_k, y_k) \mid \text{face}). \end{aligned}$$

In this case, each term of the form  $P(\text{label } k \text{ at } (x_k, y_k) \mid \text{face})$  can be learned fairly easily by labeling a large number of example images and then forming a histogram. Because the histograms are now two dimensional, the number of boxes is no longer problematic. A similar line of reasoning leads to a model of  $P(\text{image} \mid \text{no face})$ . A classifier follows from the line of reasoning given earlier. This approach has been used successfully by Schneiderman and Kanade to build detectors for faces and cars (Figure 22.5).

## 22.3 FEATURE SELECTION

Assume we have a set of pixels that we believe belong together and should be classified. What features should we present to a classifier? One approach is to present all the pixel values: This

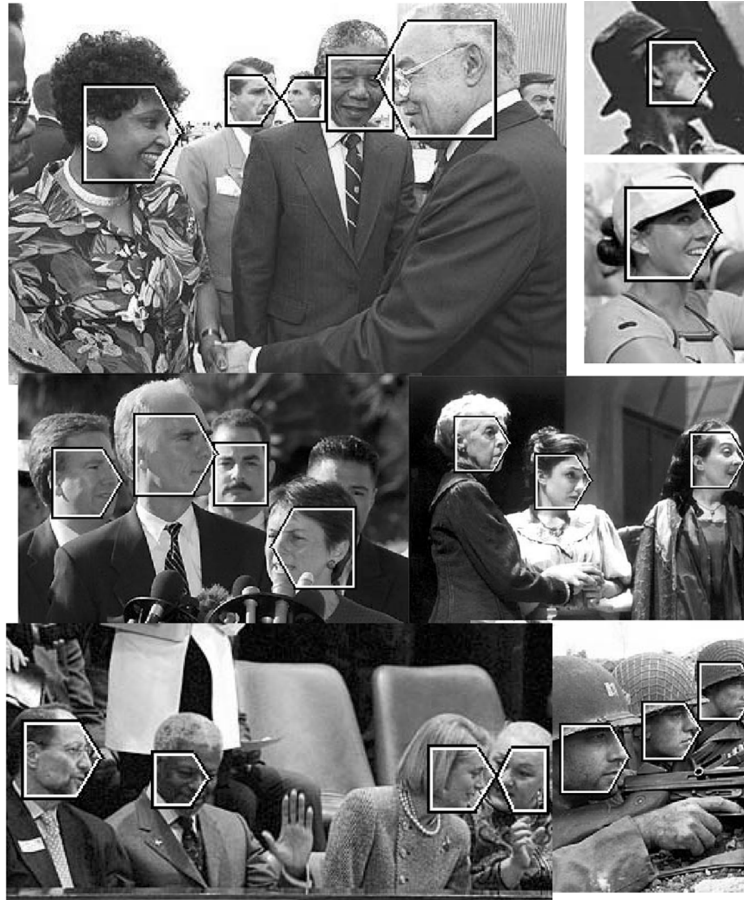


**Figure 22.5** Faces found using the method of Section 22.2.2. Image windows at various scales are classified as frontal face, lateral face, or non-face using a likelihood model learned from data. Subregions in the image window are classified into a set of classes learned from data; the face model assumes that labels from these classes are emitted independently of one another at different positions. This likelihood model yields a posterior value for each class and for each window, and the posterior value is used to identify the window. *Reprinted from A Statistical Method for 3D Object Detection Applied to Faces and Cars, H. Schneiderman and T. Kanade, Proc. Computer Vision and Pattern Recognition, 2000, © 2000, IEEE*

gives the classifier the maximum possible amount of information about the set of pixels, but creates a variety of problems.

First, high-dimensional spaces are big in the sense that large numbers of examples can be required to represent the available possibilities fairly. For example, a face at low resolution has a fairly simple structure: It consists (rather roughly) of some dark bars (the eyebrows and eyes) and light bars (the specular reflections from the nose and forehead) on a textureless background. However, if we are working with high-resolution faces, it might be difficult to supply enough examples to determine that this structure is significant and that minor variations in skin texture are irrelevant. Instead, we would like to choose a feature space that would make these properties obvious, typically by imposing some form of structure on the examples.

Second, we may know some properties of the patterns in advance. For example, we have models of the behavior of illumination. Forcing a classifier to use examples to, in essence, come up with a model that we already know is a waste of examples. We would like to use features that are consistent with our knowledge of the patterns. This might involve preprocessing regions (e.g., to remove the effects of illumination changes) or choosing features that are invariant to some kinds of transformation (e.g., scaling an image region to a standard size).

You should notice a similarity between feature selection and model selection (as described in Section 16.3). In model selection, we attempt to obtain a model that best explains a dataset; here we are attempting to find a set of features that best classifies a dataset. The two are basically the same activity in slightly distinct forms (you can view a set of features as a model and classification as explanation). Here we describe methods that are used mainly for feature selection. We concentrate on two standard methods for obtaining *linear features*—features that are a linear function of the initial feature set.

### 22.3.1 Principal Component Analysis

The core goal in feature selection is to obtain a smaller set of features that accurately represents the original set. What this means rather depends on the application. However, one important possibility is that the new set of features should capture as much of the old set's variance as possible. The easiest way to see this is to consider an extreme example. If the value of one feature can be predicted precisely from the value of the others, it is clearly redundant and can be dropped. By this argument, if we are going to drop a feature, the best one to drop is the one whose value is most accurately predicted by the others. We can do more than drop features: We can make new features as functions of the old features.

In *principal component analysis*, the new features are linear functions of the old features. In principal component analysis, we take a set of data points and construct a lower dimensional linear subspace that best explains the variation of these data points from their mean. This method (also known as the Karhunen–Loève transform) is a classical technique from statistical pattern recognition (Duda & Hart 1973, Oja 1983, Fukunaga 1990).

Assume we have a set of  $n$  feature vectors  $\mathbf{x}_i$  ( $i = 1, \dots, n$ ) in  $\mathbb{R}^d$ . The mean of this set of feature vectors is  $\boldsymbol{\mu}$  (you should think of the mean as the center of gravity in this case), and their covariance is  $\Sigma$  (you can think of the variance as a matrix of second moments). We use the mean as an origin and study the offsets from the mean ( $\mathbf{x}_i - \boldsymbol{\mu}$ ).

Our features are linear combinations of the original features; this means it is natural to consider the projection of these offsets onto various different directions. A unit vector  $\mathbf{v}$  represents a direction in the original feature space; we can interpret this direction as a new feature  $v(\mathbf{x})$ . The value of  $u$  on the  $i$ th data point is given by  $v(\mathbf{x}_i) = \mathbf{v}^T(\mathbf{x}_i - \boldsymbol{\mu})$ . A good feature captures as much of the variance of the original dataset as possible. Notice that  $v$  has zero mean; then the variance of  $v$  is

$$\begin{aligned} \text{var}(v) &= \frac{1}{n-1} \sum_{i=1}^n v(\mathbf{x}_i)v(\mathbf{x}_i)^T \\ &= \frac{1}{n} \sum_{i=1}^{n-1} \mathbf{v}^T(\mathbf{x}_i - \boldsymbol{\mu})(\mathbf{v}^T(\mathbf{x}_i - \boldsymbol{\mu}))^T \\ &= \mathbf{v}^T \left\{ \sum_{i=1}^{n-1} (\mathbf{x}_i - \boldsymbol{\mu})(\mathbf{x}_i - \boldsymbol{\mu})^T \right\} \mathbf{v} \\ &= \mathbf{v}^T \Sigma \mathbf{v}. \end{aligned}$$

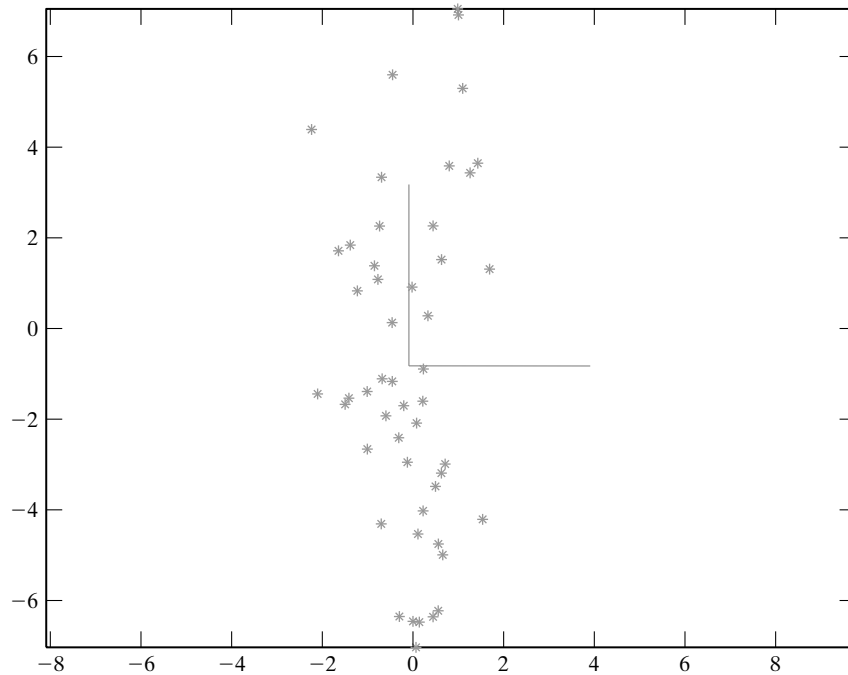


**Figure 22.6** A dataset that is well represented by a principal component analysis. The axes represent the directions obtained using PCA; the vertical axis is the first principal component, and is the direction in which the variance is highest.

Now we should like to maximize  $\mathbf{v}^T \Sigma \mathbf{v}$  subject to the constraint that  $\mathbf{v}^T \mathbf{v} = 1$ . This is an eigenvalue problem; the eigenvector of  $\Sigma$  corresponding to the largest eigenvalue is the solution. Now if we were to project the data onto a space *perpendicular* to this eigenvector, we would obtain a collection of  $d - 1$  dimensional vectors. The highest variance feature for this collection would be the eigenvector of  $\Sigma$  with second largest eigenvalue, and so on.

This means that the eigenvectors of  $\Sigma$ —which we write as  $\mathbf{v}_1, \mathbf{v}_2, \dots, \mathbf{v}_d$ , where the order is given by the size of the eigenvalue and  $\mathbf{v}_1$  has the largest eigenvalue—give a set of features with the following properties:

- They are independent (because the eigenvectors are orthogonal).
- Projection onto the basis  $\{\mathbf{v}_1, \dots, \mathbf{v}_k\}$  gives the  $k$ -dimensional set of linear features that preserves the most variance.

You should notice that, depending on the data source, principal components can give a good or a bad representation of a data set (see Figures 22.6 and 22.7, and Figure 22.9).

### 22.3.2 Identifying Individuals with Principal Components Analysis

People are extremely good at remembering and recognizing a large number of faces, and mimicking this ability in an automated computer system has a wide range of applications, including human computer interaction and security. Kanade (1973) developed the first fully automated system for face recognition, and many other approaches have since been proposed to address various instances of this problem (e.g., fixed head orientation, fixed expression etc.; see Chellappa, Wil-

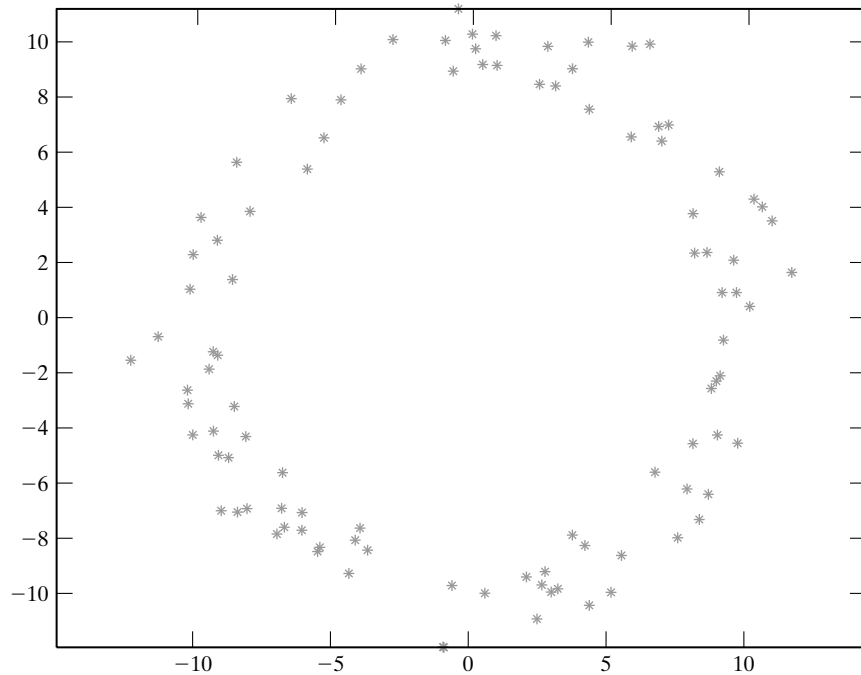


**Figure 22.7** Not every dataset is well represented by PCA. The principal components of this dataset are relatively unstable, because the variance in each direction is the same for the source. This means that we may well report significantly different principal components for different datasets from this source. This is a secondary issue—the main difficulty is that projecting the dataset onto some axis suppresses the main feature, its circular structure.

**Algorithm 22.5:** Principal components analysis identifies a collection of linear features that are independent, and capture as much variance as possible from a dataset.

Assume we have a set of  $n$  feature vectors  $\mathbf{x}_i$  ( $i = 1, \dots, n$ ) in  $\mathbb{R}^d$ . Write

$$\boldsymbol{\mu} = \frac{1}{n} \sum_i \mathbf{x}_i$$

$$\boldsymbol{\Sigma} = \frac{1}{n-1} \sum_i (\mathbf{x}_i - \boldsymbol{\mu})(\mathbf{x}_i - \boldsymbol{\mu})^T$$

The unit eigenvectors of  $\boldsymbol{\Sigma}$ —which we write as  $\mathbf{v}_1, \mathbf{v}_2, \dots, \mathbf{v}_d$ , where the order is given by the size of the eigenvalue and  $\mathbf{v}_1$  has the largest eigenvalue—give a set of features with the following properties:

- They are independent.
- Projection onto the basis  $\{\mathbf{v}_1, \dots, \mathbf{v}_k\}$  gives the  $k$ -dimensional set of linear features that preserves the most variance.

son & Sirohey 1995 for a recent survey). Finding faces typically involves either: (a) feature-based matching techniques, where facial features such as the nose, lips, eyes, and so on, are extracted and matched using their geometric parameters (height, width) and relationship (relative position); or (b) template matching methods, where the brightness patterns of two face images are directly compared (see Brunelli & Poggio 1993 for a discussion and comparison of the two approaches). However, assume a face has been found: Whose face is it? If we have a useable spatial coordinate system, PCA based methods can address this problem simply and effectively.

**Eigenpictures** People can quickly recognize enormous numbers of faces, and Sirovitch & Kirby (1987) suggested that the human visual system might only use a small number of parameters to store and index face pictures. Accordingly, they investigated the use of principal component analysis as a compression technique for face images. Indeed, PCA allows each sample  $s_i \in \mathbb{R}^d$  ( $i = 1, \dots, n$ ) to be represented by only  $p \ll d$  numbers, the coordinates of its projection in the basis formed by the vectors  $u_j$  ( $j = 1, \dots, p$ ). Of course, these vectors must also be stored, with total cost  $(n + d)p$  as opposed to the original  $nd$  storage requirement. Sirovich and Kirby dubbed the vectors  $u_i$  “eigenpictures” since they have the same dimensionality as the original images. Their experiments show that 40 eigenpictures are sufficient to reconstruct the members of an image database containing 115 128  $\times$  128 faces with a 3% error rate. Note that for these parameter values ( $p = 40$ ,  $n = 115$  and  $d = 128 \times 128$ ), the size of the eigenpicture representation (including the image projections) is less than half the size of the original database. Sirovich and Kirby also show that face images of persons who are not part of this database yield error rates inferior to 8%, even under adverse lighting conditions, which suggests an excellent extrapolating power.

**Eigenfaces** Although the idea of using eigenpictures for face recognition is implicit in their paper, Sirovich and Kirby did not propose an explicit recognition algorithm. This was done by Turk & Pentland (1991a), who presented a full recognition system based on a variant of the nearest neighbor classification scheme summarized at the beginning of this section. In the process, they renamed eigenpictures “eigenfaces.”

The recognition algorithm is divided into the following steps:

**Off-line:**

1. Collect a set of pictures of  $m$  persons reflecting variations in expression, pose, and lighting.
2. Compute the eigenfaces  $u_i$  ( $i = 1, \dots, p$ ).
3. For each person in the database, calculate the corresponding representative vector  $w_j$  ( $j = 1, \dots, m$ ) in the subspace  $V_p$  spanned by the eigenfaces.

**On-line:**

4. Compute the projection  $w$  of any new image  $t$  onto  $V_p$ .
5. If the distance  $d = |t - w|$  is greater than some preset threshold  $\varepsilon_1$ , classify the image as “non-face.”
6. Otherwise, if the minimum distance  $d_k = |w - w_k|$  between the projection of the new image and the known face representatives is smaller than some present threshold  $\varepsilon_2$ , classify the image as “person number  $k$ .”
7. In the remaining case ( $d < \varepsilon_1$  and  $d_k \geq \varepsilon_2$ ), classify the image as “unknown person”, and (optional) add the new image to the database and recompute the eigenfaces.



**Figure 22.8** A subset of the image database used in the experiments of Turk & Pentland (1991*b*). Variations in lighting, orientation and scale are also included in the actual dataset but are not shown here. Reprinted from “Face recognition using eigenfaces,” by M. Turk and A. Pentland, *Proc. Computer Vision and Pattern Recognition, 1991* © 1991, IEEE

At this point, we should clarify how the representative vectors  $w_j$  are computed (step 3). Turk and Pentland (1991*a*) propose averaging the eigenface pattern vectors, (i.e., the projections of the images associated with class number  $j$  onto  $S_p$ ). This is an alternative to the nearest-neighbor classification approach presented earlier.

In their experiments, Turk and Pentland use an image database of 2,500  $128 \times 128$  images of 16 different subjects, corresponding to all combinations of three face orientations, three head scales, and three lighting conditions (Figure 22.8).

Table 22.1 gives quantitative recognition results. In the corresponding experiments, training sets are chosen among various groups of 16 images in the original database, making sure each person appears in each training set. All images in the database are then classified. Statistics are collected by measuring the mean variation between training and test conditions. Illumination, scale, and orientation are varied independently.

**TABLE 22.1** RECOGNITION RESULTS. THE EXPERIMENTAL CONDITIONS ARE SET BY CHANGING THE VALUE OF  $\varepsilon_1$  (E.G.,  $\varepsilon_1 = +\infty$  TO FORCE CLASSIFICATION). LOWER (RESP. HIGHER) VALUES OF  $\varepsilon_1$  YIELDS MORE (RESP. LESS ) ACCURATE RECOGNITION RESULTS, BUT HIGHER (RESP. LOWER) UNKNOWN CLASSIFICATION RESULTS.

Experimental Condition	Correct/Unknown Recognition Percentage		
	Lighting	Orientation	Scale
Forced classification	96/0	85/0	64/0
Forced 100% accuracy	100/19	100/39	100/60
Forced 20% unknown rate	100/20	94/20	74/20



### 22.3.3 Canonical Variates

Principal component analysis yields a set of linear features of a particular dimension that best represents the variance in a high-dimensional dataset. There is no guarantee that this set of features is good for *classification*. For example, Figure 22.9 shows a dataset where the first principal component would yield a bad classifier, and the second principal component would yield quite a good one, despite not capturing the variance of the dataset.

Linear features that emphasize the distinction between classes are known as *canonical variates*. To construct canonical variates, assume that we have a set of data items  $\mathbf{x}_i$ , for  $i \in \{1, \dots, n\}$ . We assume that there are  $p$  features (i.e., that the  $\mathbf{x}_i$  are  $p$ -dimensional vectors). We

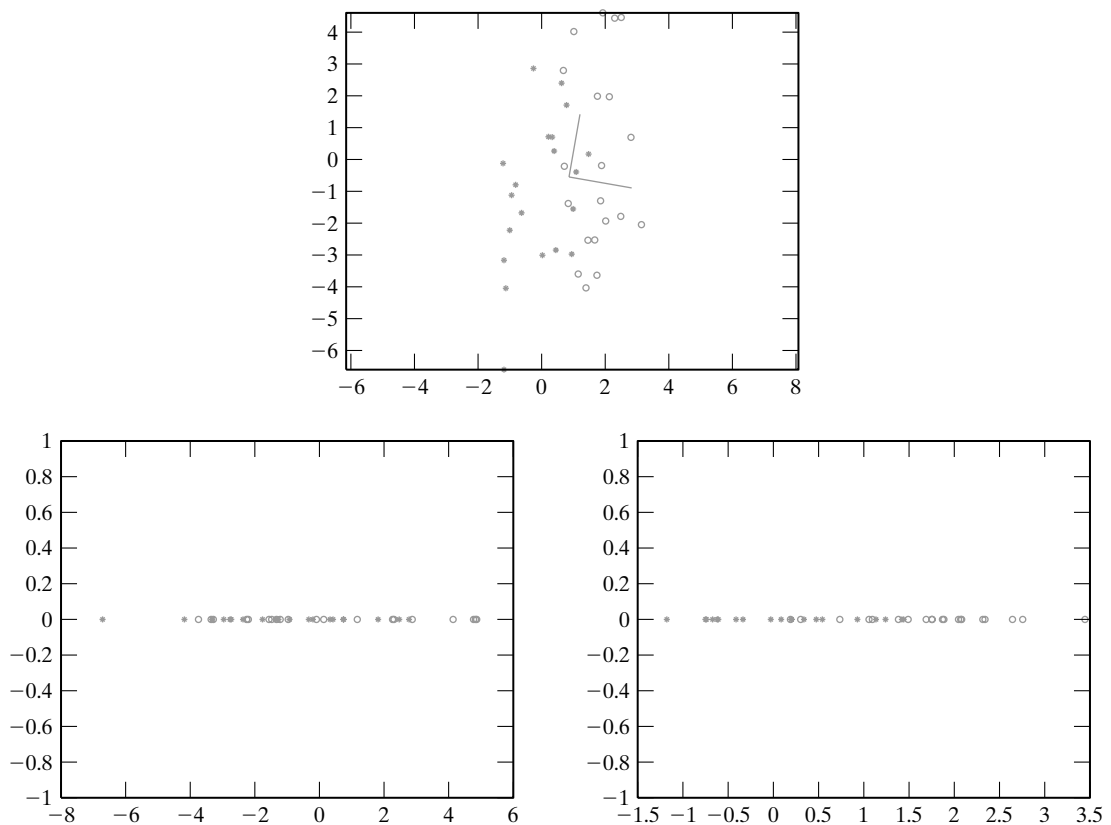


**Figure 22.9** Principal component analysis doesn't take into account the fact that there may be more than one class of item in a dataset. This can lead to significant problems. For a classifier, we would like to obtain a set of features that reduces the number of features and makes the difference between classes most obvious. For the dataset on the **top**, one class is indicated by circles and the other by stars. PCA would suggest projection onto a vertical axis, which captures the variance in the dataset, but cannot be used to discriminate it as we can see from the axes obtained by PCA, which are overlaid on the dataset. The **bottom row** shows the projections onto those axes. On the **bottom left**, we show the projection onto the first principal component, which has higher variance but separates the classes poorly, and on the **bottom right**, we show the projection onto the second principal component, which has significantly lower variance (look at the axes) and gives better separation.



have  $g$  different classes, and the  $j$ th class has mean  $\mu_j$ . Write  $\bar{\mu}$  for the mean of the class means, that is,

$$\bar{\mu} = \frac{1}{g} \sum_{j=1}^g \mu_j,$$

Write

$$\mathcal{B} = \frac{1}{g-1} \sum_{j=1}^g (\mu_j - \bar{\mu})(\mu_j - \bar{\mu})^T.$$

Note that  $\mathcal{B}$  gives the variance of the class means. In the simplest case, we assume that each class has the same covariance  $\Sigma$ , and that this has full rank. We would like to obtain a set of axes where the clusters of data points belonging to a particular class group together tightly, whereas the distinct classes are widely separated. This involves finding a set of features that maximizes the ratio of the separation (variance) between the class means to the variance within each class. The separation between the class means is typically referred to as the *between-class variance*, and the variance within a class is typically referred to as the *within-class variance*.

Now we are interested in linear functions of the features, so we concentrate on

$$v(x) = v^T x.$$

We should like to maximize the ratio of the between-class variances to the within-class variances for  $v_1$ .

Using the same argument as for principal components, we can achieve this by choosing  $v$  to maximize

$$\frac{v_1^T \mathcal{B} v_1}{v_1^T \Sigma v_1}.$$

This problem is the same as maximizing  $v_1^T \mathcal{B} v_1$  subject to the constraint that  $v_1^T \Sigma v_1 = 1$ . In turn, a solution has the property that

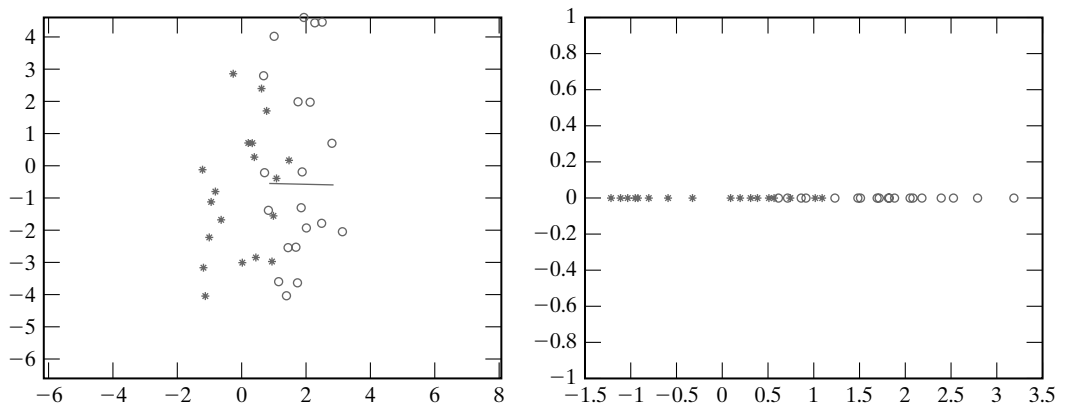


**Figure 22.10** Canonical variates use the class of each data item as well as the features in estimating a good set of linear features. In particular, the approach constructs axes that separate different classes as well as possible. The dataset used in Figure 22.9 is shown on the **left**, with the axis given by the first canonical variate overlaid. On the **bottom right**, we show the projection onto that axis, where the classes are rather well separated.

$$\mathcal{B}\mathbf{v}_1 + \lambda\Sigma\mathbf{v}_1 = 0$$

for some constant  $\lambda$ . This is known as a *generalized eigenvalue problem*—if  $\Sigma$  has full rank, we can solve it by finding the eigenvector of  $\Sigma^{-1}\mathcal{B}$  with largest eigenvalue (otherwise we use specialized routines within the relevant numerical software environment).

Now for each  $\mathbf{v}_l$ , for  $2 \leq l \leq p$ , we should like to find features that extremize the criterion and are independent of the the previous  $\mathbf{v}_l$ . These are provided by the other eigenvectors of  $\Sigma^{-1}\mathcal{B}$ . The eigenvalues give the variance along the features (which are independent). By choosing the  $m < p$  eigenvectors with the largest eigenvalues, we obtain a set of features that reduces the dimension of the feature space while best preserving the separation between classes. This doesn't guarantee the best error rate for a classifier on a reduced number of features, but it offers a good place to start by reducing the number of features while respecting the category structure (Figure 22.11). Details and examples appear in McLachlan & Krishnan (1996), or in Ripley (1996).

**Algorithm 22.6:** *Canonical variates* identifies a collection of linear features that separating the classes as well as possible

Assume that we have a set of data items of  $g$  different classes. There are  $n_k$  items in each class, and a data item from the  $k$ th class is  $\mathbf{x}_{k,i}$ , for  $i \in \{1, \dots, n_k\}$ . The  $j$ th class has mean  $\boldsymbol{\mu}_j$ . We assume that there are  $p$  features (i.e., that the  $\mathbf{x}_i$  are  $p$ -dimensional vectors).

Write  $\bar{\boldsymbol{\mu}}$  for the mean of the class means, that is,

$$\bar{\boldsymbol{\mu}} = \frac{1}{g} \sum_{j=1}^g \boldsymbol{\mu}_j,$$

Write

$$\mathcal{B} = \frac{1}{g-1} \sum_{j=1}^g (\boldsymbol{\mu}_j - \bar{\boldsymbol{\mu}})(\boldsymbol{\mu}_j - \bar{\boldsymbol{\mu}})^T.$$

Assume that each class has the same covariance  $\Sigma$ , which is either known or estimated as

$$\Sigma = \frac{1}{N-1} \sum_{c=1}^g \left\{ \sum_{i=1}^{n_c} (\mathbf{x}_{c,i} - \boldsymbol{\mu}_c)(\mathbf{x}_{c,i} - \boldsymbol{\mu}_c)^T \right\}.$$

The unit eigenvectors of  $\Sigma^{-1}\mathcal{B}$ , which we write as  $\mathbf{v}_1, \mathbf{v}_2, \dots, \mathbf{v}_d$ , where the order is given by the size of the eigenvalue and  $\mathbf{v}_1$  has the largest eigenvalue, give a set of features with the following property:

- Projection onto the basis  $\{\mathbf{v}_1, \dots, \mathbf{v}_k\}$  gives the  $k$ -dimensional set of linear features that best separates the class means.

If the classes don't have the same covariance, it is still possible to construct canonical variates. In this case, we estimate a  $\Sigma$  as the covariance of all the offsets of each data item *from its own class mean* and proceed as before. Again, this is an approach without a guarantee of optimality, but one that can work quite well in practice.

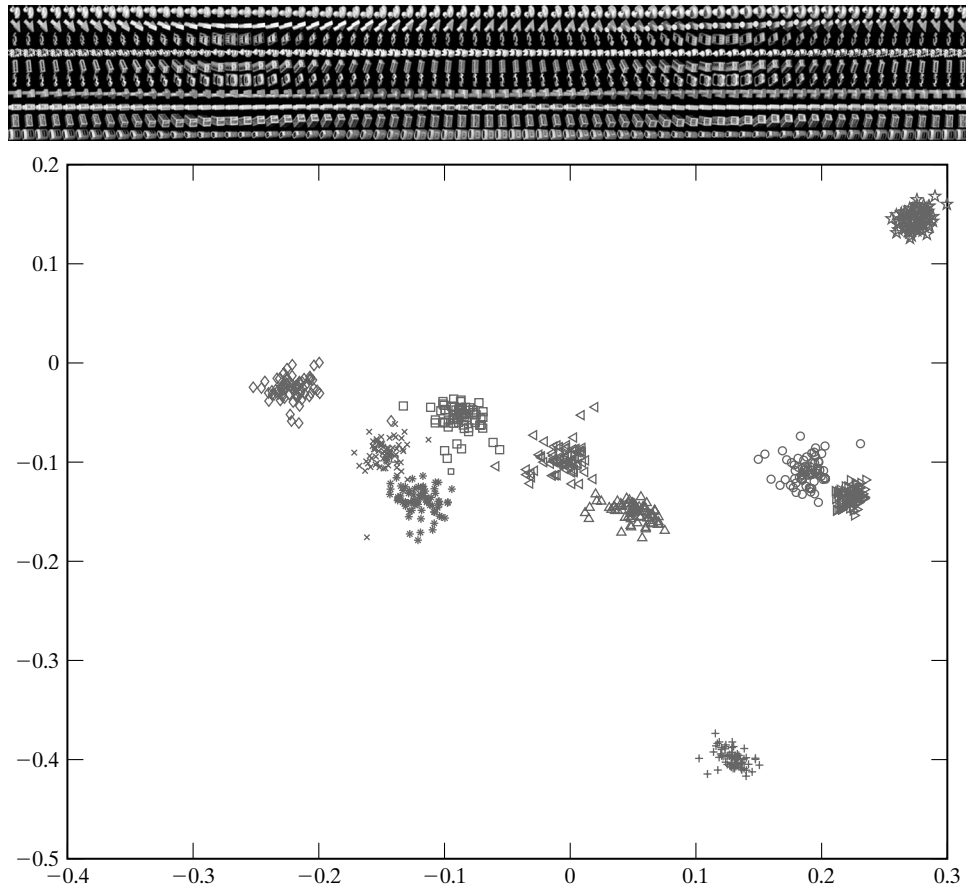


**Figure 22.11** Canonical variates are effective for a variety of simple template matching problems. The figure on top shows views of 10 objects at a variety of poses on a black background (these images are smoothed and resampled versions of images in the well-known COIL database due to Nene and Nayar and available at <http://www.cs.columbia.edu/CAVE/research/softlib/coil-20.html>—a version with 20 objects—or <http://www.cs.columbia.edu/CAVE/research/softlib/coil-100.html>—a version with 100 objects) Identifying an object from one of these images is a relatively simple matter because objects appear on a constant background; they do not need to be segmented. We then used 60 of the images of each object to determine a set of canonical variates. The figure below shows the first two canonical variates for 71 images—the 60 training images and 11 others—of each object (different symbols correspond to different objects). Note that the clusters are tight and well separated; on these two canonical variates alone, we could probably get quite good classification.

## 22.4 NEURAL NETWORKS

It is commonly the case that neither simple parametric density models nor histogram models can be used. In this case, we must either use more sophisticated density models (an idea we explore in this section) or look for decision boundaries directly (Section 22.5).

### 22.4.1 Key Ideas

A *neural network* is a parametric approximation technique that has proved useful for building density models. Neural networks typically approximate a vector function  $f$  of some input  $x$  with a series of *layers*. Each layer forms a vector of outputs each of which is obtained by applying the same nonlinear function, which we write as  $\phi$ , to different affine functions of the inputs. We adopt the convenient trick of adding an extra component to the inputs and fixing the value of this component at one so we obtain a linear function of this augmented input vector. This means that a layer with augmented input vector  $u$  and output vector  $v$  can be written as

$$v = [\phi(w_1 \cdot u), \phi(w_2 \cdot u), \dots, \phi(w_n \cdot u)],$$

where the  $w_i$  are parameters that can be adjusted to approve the approximation.

Typically, a neural net uses a sequence of layers to approximate a function. Each layer uses augmented input vectors. For example, if we are approximating a vector function  $g$  of a vector  $x$  with a two layer net, we obtain

$$g(x) \approx f(x) = [\phi(w_{21} \cdot y), \phi(w_{22} \cdot y), \dots, \phi(w_{2n} \cdot y)],$$

where

$$y(z) = [\phi(w_{11} \cdot z), \phi(w_{12} \cdot z), \dots, \phi(w_{1m} \cdot z), 1]$$

and

$$z(x) = [x_1, x_2, \dots, x_p, 1].$$

Some of the elements of  $w_{1k}$  or  $w_{2k}$  could be clamped at zero; in this case, we are insisting that some elements of  $y$  do not affect  $f(x)$ . If this is the case, the layer is referred to as a *partially connected layer*; otherwise it is known as a *fully connected layer*. Of course, layer two could be either fully or partially connected as well. The parameter  $n$  is fixed by the dimension of  $f$  and  $p$  is fixed by the dimension of  $x$ , but there is no reason that  $m$  should be the same as either  $n$  or  $p$ . Typically,  $m$  is larger than either. A similar construction yields three layer networks (or networks with more layers, which are uncommon). Neural networks are often drawn with circles indicating variables and arrows indicating possibly nonzero connections; this gives a representation that exposes the basic structure of the approximation (Figure 22.12).

**Choosing a Nonlinearity** There are a variety of possibilities for  $\phi$ . For example, we could use a *threshold function*, which has value one when the argument is positive and zero otherwise. It is quite easy to visualize the response of a layer of that uses a threshold function; each component of the layer changes from zero to one along a hyperplane. This means that the output vector takes different values in each cell of an arrangement of hyperplanes in the input space. Networks that use layers of this form are hard to train, because the threshold function is not differentiable.

It is more common to use a  $\phi$  that changes smoothly (but rather quickly) from zero to one, often called a *sigmoid function* or *squashing function*. The *logistic function* is one popular example. This is a function of the form

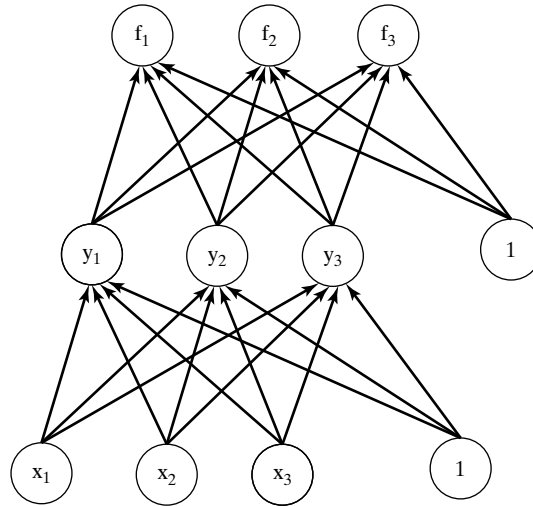


**Figure 22.12** Neural networks are often illustrated by diagrams of the form shown here. Each circle represents a variable, and the circles are typically labeled with the variable. The “layers” are obvious in such a drawing. This network is the two-layer network given in the text; the arrows indicate that the coefficient coupling the two variables in the affine function could be nonzero. This network is fully connected because all arrows are present. It is possible to have arrows skip layers.

$$\phi(x; \nu) = \frac{e^{x/\nu}}{1 + e^{x/\nu}},$$

where  $\nu$  controls how sharply the function changes at  $x = 0$ . It isn’t crucial that the horizontal asymptotes are zero and one. Another popular squashing function is

$$\phi(x; \nu, A) = A \tanh(\nu x),$$

which has horizontal asymptotes at  $A$  and  $-A$ . Figure 22.13 illustrates these nonlinearities.

**Producing a Classifier Using a Neural Net** To produce a neural net that approximates some function  $\mathbf{g}(\mathbf{x})$ , we collect a series of examples  $\mathbf{x}^e$ . We construct a network that has one output for each dimension of  $\mathbf{g}$ . Write this network as  $\mathbf{n}(\mathbf{x}; \mathbf{p})$ , where  $\mathbf{p}$  is a parameter vector that contains all the  $w_{ij}$ . We supply a desired output vector  $\mathbf{o}^e$  for this input; typically,  $\mathbf{o}^e = \mathbf{g}(\mathbf{x}^e)$ . We now obtain  $\hat{\mathbf{p}}$  that minimizes

$$Error(\mathbf{p}) = \left(\frac{1}{2}\right) \sum_e |\mathbf{n}(\mathbf{x}^e; \mathbf{p}) - \mathbf{o}^e|^2$$

using appropriate optimization software (the half simplifies a little notation later on, but is of no real consequence).

The most significant case occurs when  $\mathbf{g}(\mathbf{x})$  is intended to approximate the posterior on classes given the data. We do not know this posterior, and so cannot supply its value to the training procedure. Instead, we require that our network has one output for each class. Given an example  $\mathbf{x}^e$ , we construct a desired output  $\mathbf{o}^e$  as a vector that contains a one in the component corresponding to that example’s class and a zero in each other component. We now train the net as before, and regard the output of the neural network as a model of the posterior probability. An

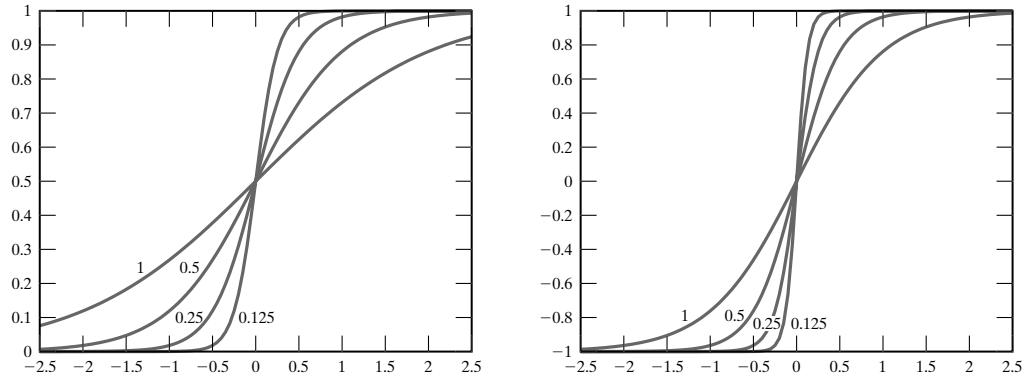


**Figure 22.13** On the **left**, a series of squashing functions obtained using  $\phi(x; \nu) = \frac{e^{x/\nu}}{1+e^{x/\nu}}$ , for different values of  $\nu$  indicated on the figure. On the **right**, a series of squashing functions obtained using  $\phi(x; \nu, A) = A \tanh(x/\nu)$  for different values of  $\nu$  indicated on the figure. Generally, for  $x$  close to the center of the range, the squashing function is linear; for  $x$  small or large, it is strongly nonlinear.

input  $\mathbf{x}$  is then classified by forming  $\mathbf{n}(\mathbf{x}; \hat{\mathbf{p}})$ , and then choosing the class that corresponds to the largest component of this vector.

### 22.4.2 Minimizing the Error

Recall that we are training a net by minimizing the sum over the examples of the difference between the desired output and the actual output, that is, by minimizing

$$Error(\mathbf{p}) = \left(\frac{1}{2}\right) \sum_e |\mathbf{n}(\mathbf{x}^e; \mathbf{p}) - \mathbf{o}^e|^2$$

as a function of the parameters  $\mathbf{p}$ . There are a variety of strategies for obtaining  $\hat{\mathbf{p}}$ , the set of parameters that minimize this error. One is gradient descent; from some initial point  $\mathbf{p}_i$ , we compute a new point  $\mathbf{p}_{i+1}$  by

$$\mathbf{p}_{i+1} = \mathbf{p}_i - \epsilon(\nabla Error),$$

where  $\epsilon$  is some small constant.

**Stochastic Gradient Descent** Write the error for example  $e$  as  $Error(\mathbf{p}; \mathbf{x}^e)$  so the total error is  $Error(\mathbf{p}) = \sum_e Error(\mathbf{p}; \mathbf{x}^e)$ . Now if we use gradient descent, we are updating parameters using the algorithm

$$\mathbf{p}_{i+1} = \mathbf{p}_i - \epsilon \nabla Error$$

(where the gradient is with respect to  $\mathbf{p}$  and is evaluated at  $\mathbf{p}_i$ ). This works because, if  $\epsilon$  is sufficiently small, we have

$$\begin{aligned} Error(\mathbf{p}_{i+1}) &= Error(\mathbf{p}_i - \epsilon \nabla Error) \\ &\approx Error(\mathbf{p}_i) - \epsilon(\nabla Error \cdot \nabla Error) \\ &\leq Error(\mathbf{p}_i), \end{aligned}$$

with equality only at an extremum. This creates a problem: Evaluating the error and its gradient is going to involve a sum over all examples, which may be a large number. We should like to avoid this sum; it turns out that it is possible to do so by selecting an example at random, computing the gradient *for that example alone*, and updating the parameters using that gradient. In this process, known as *stochastic gradient descent*, we update the parameters using the algorithm

$$\mathbf{p}_{i+1} = \mathbf{p}_i - \epsilon \nabla \text{Error}(\mathbf{p}; \mathbf{x}^e)$$

(where the gradient is with respect to  $\mathbf{p}$ , is evaluated at  $\mathbf{p}_i$ , and we choose the example uniformly at random, making a different choice at each step). In this case, the error doesn't necessarily go down for each particular choice, but the *expected* value of the error *does* go down for a sufficiently small value of  $\epsilon$ . In particular, we have

$$\begin{aligned} \text{E}(\text{Error}(\mathbf{p}_{i+1})) &= \text{E}(\text{Error}(\mathbf{p}_i - \epsilon \nabla \text{Error}(\mathbf{p}; \mathbf{x}^e))) \\ &\approx \text{E}(\text{Error}(\mathbf{p}_i) - \epsilon (\nabla \text{Error} \cdot \nabla \text{Error}(\mathbf{p}; \mathbf{x}^e))) \\ &= \text{Error}(\mathbf{p}_i) - \epsilon \frac{1}{n} \sum_e (\nabla \text{Error} \cdot \nabla \text{Error}(\mathbf{p}; \mathbf{x}^e)) \\ &= \text{Error}(\mathbf{p}_i) - \epsilon \left( \nabla \text{Error} \cdot \left( \frac{1}{n} \sum_e \nabla \text{Error}(\mathbf{p}; \mathbf{x}^e) \right) \right) \\ &= \text{Error}(\mathbf{p}_i) - \frac{\epsilon}{n} (\nabla \text{Error} \cdot \nabla \text{Error}) \\ &< \text{Error}(\mathbf{p}_i) \text{ if } |\nabla E| > 0. \end{aligned}$$

By taking sufficient steps down a gradient computed using only one example (selected uniformly and at random each time we take a step), we can in fact minimize the function. This is because the expected value goes down for each step unless we're at the minimum. The gradient can be computed in a number of ways; one efficient trick is *backpropagation*, described in Section 22.7.

**Algorithm 22.7:** *Stochastic gradient descent* minimizes the error of a neural net approximation using backpropagation to compute the derivatives

```

Choose  $\mathbf{p}_o$  (randomly)
Use backpropagation (Algorithm 22.9) to compute
 $\nabla \text{Error}(\mathbf{x}^e; \mathbf{p}_o)$ 
 $\mathbf{p}_n = \mathbf{p}_o - \epsilon \nabla \text{Error}(\mathbf{x}^e; \mathbf{p}_o)$ 
Until  $|\text{Error}(\mathbf{p}_n) - \text{Error}(\mathbf{p}_o)|$  is small
or  $|\mathbf{p}_o - \mathbf{p}_n|$  is small

 $\mathbf{p}_o = \mathbf{p}_n$ 
Choose an example  $(\mathbf{x}^e, \mathbf{o}^e)$  uniformly and
at random from the training set
Use backpropagation (Algorithm 22.9) to compute
 $\nabla \text{Error}(\mathbf{x}^e; \mathbf{p}_o)$ 
 $\mathbf{p}_n = \mathbf{p}_o - \epsilon \nabla \text{Error}(\mathbf{x}^e; \mathbf{p}_o)$ 
end

```

### 22.4.3 When to Stop Training

Typically, gradient descent is not continued until an exact minimum is found. Surprisingly, this is a source of robustness. The easiest way to understand this is to consider the shape of the error function around the minimum. If the error function changes sharply at the minimum, then the performance of the network is quite sensitive to the choice of parameters. This suggests that the network generalizes badly. You can see this by assuming that the training examples are one half of a larger set; if we had trained the net on the other half we'd have obtained slightly different set of parameters. This means that the net with our current parameters will perform badly on this other half, because the error changes sharply with a small change in the parameters.

Now if the error function doesn't change sharply at the minimum, there is no particular point in expending effort to be at the minimum value as long as we are reasonably close—we know that this minimum error value won't be attained on a training set. It is common practice to continue with stochastic gradient descent until (a) each example has been visited on average rather more than once, and (b) the decrease in the value of the function goes below some threshold.

A more difficult question is how many layers to use and how many units to use in each layer. This question, which is one of model selection, tends to be resolved by experiment. We refer interested readers to Ripley (1996) and Haykin (1999).

### 22.4.4 Finding Faces Using Neural Networks

Face finding is an application that illustrates the usefulness of classifiers. In frontal views at a fairly coarse scale, all faces look basically the same. There are bright regions on the forehead, the cheeks, and the nose, and dark regions around the eyes, the eyebrows, the base of the nose, and the mouth. This suggests approaching face finding as a search over all image windows of a fixed size for windows that look like a face. Larger or smaller faces can be found by searching coarser or finer scale images.

Because a face illuminated from the left looks different than a face illuminated from the right, the image windows must be corrected for illumination. Generally, illumination effects look enough like a linear ramp (one side is bright, the other side is dark, and there is a smooth transition between them) that we can simply fit a linear ramp to the intensity values and subtract that from the image window. Another way to do this would be to log-transform the image and then subtract a linear ramp fitted to the logs. This has the advantage that (using a rather rough model) illumination effects are additive in the log transform. There doesn't appear to be any evidence in the literature that the log transform makes much difference in practice. Another approach is to histogram equalize the window to ensure that its histogram is the same as that of a set of reference images (histogram equalisation is described in Figure 22.14).

Once the windows have been corrected for illumination, we need to determine whether there is a face present. The orientation isn't known, and so we must either determine it or produce a classifier that is insensitive to orientation. Rowley, Baluja & Kanade (1998*b*) produced a face finder that finds faces very successfully by firstly estimating the orientation of the window, using one neural net, and then reorienting the window so that it is frontal, and passing the frontal window onto another neural net (see Figure 22.15; the paper is a development of Rowley, Baluja & Kanade 1996 and 1998*a*). The orientation finder has 36 output units, each coding for a  $10^\circ$  range of orientations; the window is reoriented to the orientation given by the largest output. Examples of the output of this system are given in Figure 22.16.



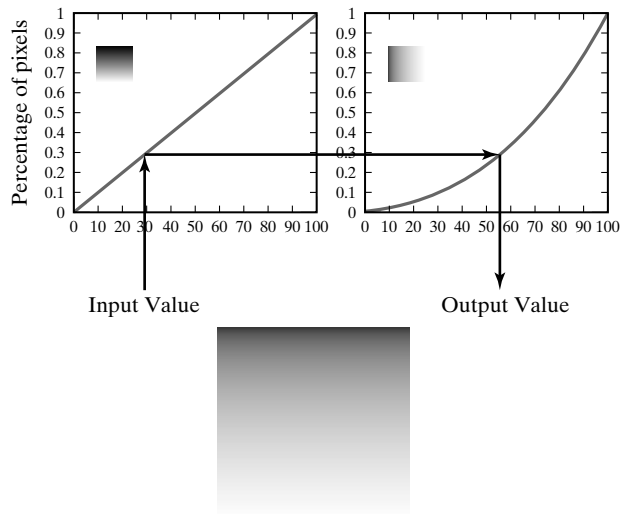


**Figure 22.14** Histogram equalization uses cumulative histograms to map the gray levels of one image so that it has the same histogram as another image. The figure at the top shows two cumulative histograms with the relevant images inset in the graphs. To transform the left image so that it has the same histogram as the right image, we take a value from the left image, read off the percentage from the cumulative histogram of that image, and obtain a new value for that gray level from the inverse cumulative histogram of the right image. The image on the left is a linear ramp (it looks nonlinear because the relationship between brightness and lightness is not linear); the image on the right is a cube root ramp. The result—the linear ramp, with gray levels remapped so that it has the same histogram as the cube root ramp—is shown on the bottom row.

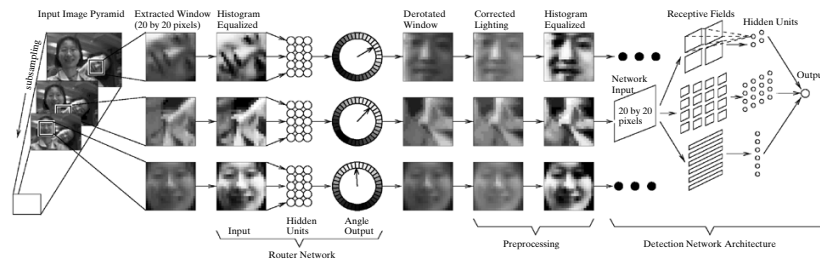


**Figure 22.15** The architecture of Rowley, Baluja, and Kanade’s system for finding faces. Image windows of a fixed size are corrected to a standard illumination using histogram equalization; they are then passed to a neural net that estimates the orientation of the window. The windows are reoriented and passed to a second net that determines whether a face is present. *Reprinted from “Rotation invariant neural-network based face detection,” by H.A. Rowley, S. Baluja and T. Kanade, Proc. Computer Vision and Pattern Recognition, 1998, © 1998, IEEE*



**Figure 22.16** Typical responses for the Rowley, Baluja, and Kanade system for face finding; a mask icon is superimposed on each window that is determined to contain a face. The orientation of the face is indicated by the configuration of the eye holes in the mask. *Reprinted from "Rotation invariant neural-network based face detection," by H.A. Rowley, S. Baluja and T. Kanade, Proc. Computer Vision and Pattern Recognition, 1998, © 1998, IEEE*

### 22.4.5 Convolutional Neural Nets

Neural networks are not confined to the architecture sketched before; there is a wide variety of alternatives (a good start is to look at Bishop 1995 or at Haykin 1999). One architecture that has proved useful in vision applications is the *convolutional neural network*. The motivating idea here is that it appears to be useful to represent image regions with filter outputs. Furthermore, we can obtain a compositional representation we apply filters to a representation itself obtained using filter outputs. For example, assume that we are looking for handwritten characters; the

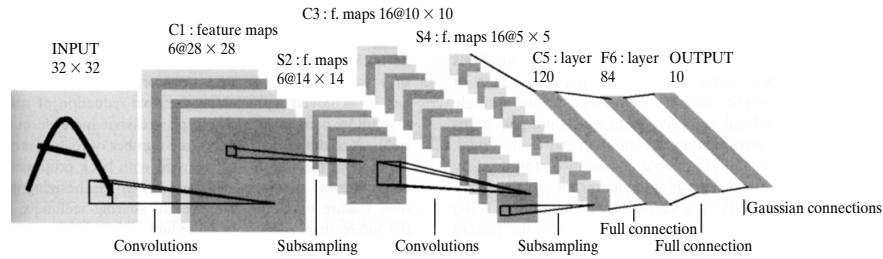


**Figure 22.17** The architecture of LeNet 5, a convolutional neural net used for recognizing handwritten characters. The layers marked C are convolutional layers; those marked S are subsampling layers. The general form of the classifier uses an increasing number of features at increasingly coarse scales to represent the image window. Finally, the window is passed to a fully connected neural net, which produces a rectified output that is classified by looking at its distance from a set of canonical templates for characters. *Figure from “Gradient-Based Learning Applied to Document Recognition,” by Y. Lecun et al. Proc. IEEE, 1998 © 1998, IEEE*

response of oriented bar filters is likely to be useful here. If we obtain a map of the oriented bars in the image, we can apply another filter to this map, and the output of this filter indicates spatial relations between the bars.

These observations suggest using a system of filters to build up a set of relations between primitives, and then using a conventional neural network to classify on the resulting representation. There is no particular reason to specify the filters in advance; instead, we could learn them, too.

Lecun, Bottou, Bengio & Haffner (1998) built a number of classifiers for handwritten digits using a convolutional neural network (Lecun et al. 1998). The basic architecture is given in Figure 22.17. The classifier is applied to a  $32 \times 32$  image window. The first stage, C1 in the figure, consists of six feature maps. The feature maps are obtained by convolving the image with a  $5 \times 5$  filter kernel, adding a constant, and applying a sigmoid function. Each map uses a different kernel and constant, and these parameters are learned.

Because the exact position of a feature should not be important, the resolution of the feature maps is reduced, leading to a new set of six feature maps—S2 in the figure. These maps are subsampled versions of the previous layer; this subsampling is achieved by averaging  $2 \times 2$  neighborhoods, multiplying by a parameter, adding a parameter, and passing the result through a sigmoid function. The multiplicative and additive parameters are learned. A series of pairs of layers of this form follows, with the number of feature maps increasing as the resolution decreases. Finally, there is a layer with 84 outputs; each of these outputs is supplied by a unit that takes every element of the previous layer as an input.

This network is used to recognize hand printed characters. The outputs are seen as a  $7 \times 12$  image of a character that has been rectified from its hand-printed version, and can now be compared with a canonical pattern for that character. The network can rectify distorted characters successfully. The input character is given the class of the character whose canonical pattern is closest to the rectified version. The resulting network has a test error rate of 0.95% (Figure 22.18).

## 22.5 THE SUPPORT VECTOR MACHINE

From the perspective of the vision community, classifiers are not an end in themselves, but a means. Thus, when a technique that is simple, reliable, and effective becomes available, it tends to

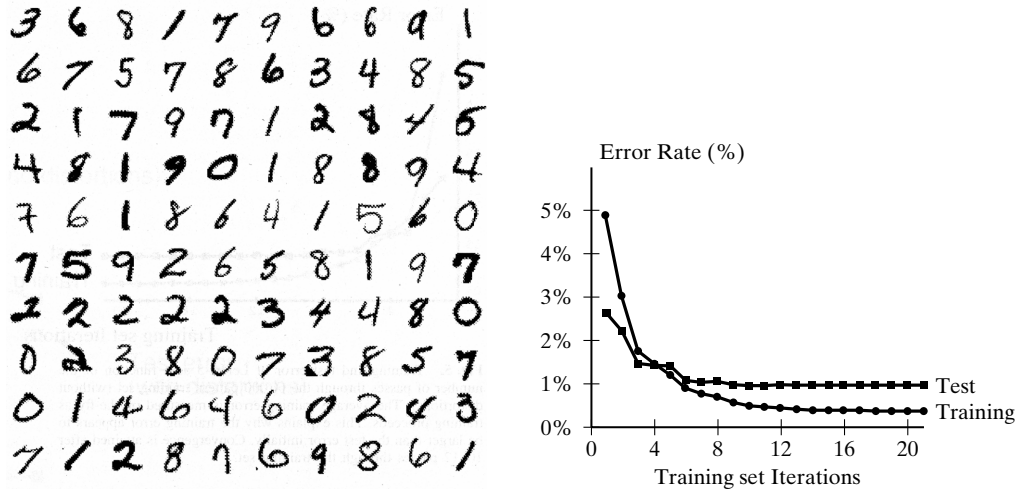


**Figure 22.18** On the left, a small subset of the MNIST database of handwritten characters used to train and test LeNet 5. Note the fairly wide variation in the appearance of each character. On the right, the error rate of LeNet 5 on a training set and on a test set, plotted as a function of the number of gradient descent passes through the entire training set of 60,000 examples (i.e., if the horizontal axis reads six, the training has taken 360,000 gradient descent steps). Note that at some point the training error goes down but the test error doesn't; this phenomenon occurs because the system's performance is optimized on the training data. A substantial difference would indicate overfitting. *Figure from "Gradient-Based Learning Applied to Document Recognition," by Y. Lecun et al. Proc. IEEE, 1998 © 1998, IEEE*

be adopted quite widely. The *support vector machine* is such a technique. This should be the first classifier you think of when you wish to build a classifier from examples (unless the examples come from a known distribution, which hardly ever happens). We give a basic introduction to the ideas, and show some examples where the technique has proved useful.

Assume we have a set of  $N$  points  $x_i$  that belong to two classes, which we indicate by 1 and  $-1$ . These points come with their class labels, which we write as  $y_i$ ; thus, our dataset can be written as

$$\{(x_1, y_1), \dots, (x_N, y_N)\}.$$

We should like to determine a rule that predicts the sign of  $y$  for any point  $x$ ; this rule is our classifier.

At this point, we distinguish between two cases: Either the data is linearly separable, or it isn't. The linearly separable case is much easier, and we deal with it first.

### 22.5.1 Support Vector Machines for Linearly Separable Datasets

In a linearly separable dataset, there is some choice of  $w$  and  $b$  (which represent a hyperplane) such that

$$y_i (w \cdot x_i + b) > 0$$

for every example point (notice the devious use of the sign of  $y_i$ ). There is one of these expressions for each data point, and the set of expressions represents a set of constraints on the choice of  $\mathbf{w}$  and  $b$ . These constraints express the constraint that all examples with a negative  $y_i$  should be on one side of the hyperplane and all with a positive  $y_i$  should be on the other side.

In fact, because the set of examples is finite, there is a family of separating hyperplanes. Each of these hyperplanes must separate the convex hull of one set of examples from the convex hull of the other set of examples. The most conservative choice of hyperplane is the one that is furthest from both hulls. This is obtained by joining the closest points on the two hulls, and constructing a hyperplane perpendicular to this line and through its midpoint. This hyperplane is as far as possible from each set, in the sense that it maximizes the minimum distance from example points to the hyperplane (Figure 22.19).

Now we can choose the scale of  $\mathbf{w}$  and  $b$  because scaling the two together by a positive number doesn't affect the validity of the constraints  $y_i(\mathbf{w} \cdot \mathbf{x}_i + b) > 0$ . This means that we can choose  $\mathbf{w}$  and  $b$  such that for every data point we have

$$y_i (\mathbf{w} \cdot \mathbf{x}_i + b) \geq 1$$

and such that equality is achieved on at least one point on each side of the hyperplane. Now assume that  $\mathbf{x}_k$  achieves equality and  $y_k = 1$ , and  $\mathbf{x}_l$  achieves equality and  $y_l = -1$ . This means that  $\mathbf{x}_k$  is on one side of the hyperplane and  $\mathbf{x}_l$  is on the other. Furthermore, the distance from  $\mathbf{x}_l$

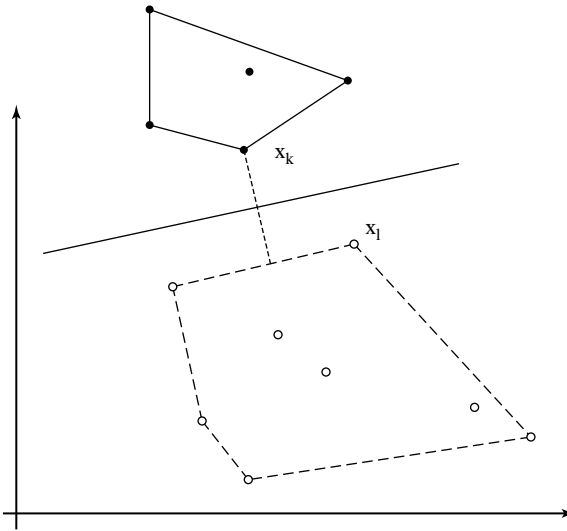


**Figure 22.19** The hyperplane constructed by a support vector classifier for a plane dataset. The filled circles are data points corresponding to one class, and the empty circles are data points corresponding to the other. We have drawn in the convex hull of each dataset. The most conservative choice of hyperplane is one that maximizes the minimum distance from each hull to the hyperplane. A hyperplane with this property is obtained by constructing the shortest line segment between the hulls and then obtaining a hyperplane perpendicular to this line segment and through its midpoint. Only a subset of the data determines the hyperplane. Of particular interest are points on each convex hull that are associated with a minimum distance between the hulls. We use these points to find the hyperplane in the text.

to the hyperplane is minimal (among the points on the same side as  $\mathbf{x}_l$ ) as is the distance from  $\mathbf{x}_k$  to the hyperplane. Notice that there might be several points with these properties.

This means that  $\mathbf{w} \cdot (\mathbf{x}_1 - \mathbf{x}_2) = 2$ , so that

$$\begin{aligned} \text{dist}(\mathbf{x}_k, \text{hyperplane}) + \text{dist}(\mathbf{x}_l, \text{hyperplane}) &= \left( \frac{\mathbf{w}}{|\mathbf{w}|} \cdot \mathbf{x}_k + \frac{b}{|\mathbf{w}|} \right) - \left( \frac{\mathbf{w}}{|\mathbf{w}|} \cdot \mathbf{x}_l + \frac{b}{|\mathbf{w}|} \right) \\ &= \frac{\mathbf{w}}{|\mathbf{w}|} \cdot (\mathbf{x}_1 - \mathbf{x}_2) = \frac{2}{|\mathbf{w}|}. \end{aligned}$$

This means that maximizing the distance is the same as *minimizing*  $(1/2)\mathbf{w} \cdot \mathbf{w}$ . We now have the constrained minimization problem:

$$\begin{aligned} &\text{minimize } (1/2)\mathbf{w} \cdot \mathbf{w} \\ &\text{subject to } y_i (\mathbf{w} \cdot \mathbf{x}_i + b) \geq 1, \end{aligned}$$

where there is one constraint for each data point.

**Solving for the Support Vector Machine** We can solve this problem by introducing Lagrange multipliers  $\alpha_i$  to obtain the Lagrangian

$$(1/2)\mathbf{w} \cdot \mathbf{w} - \sum_1^N \alpha_i (y_i (\mathbf{w} \cdot \mathbf{x}_i + b) - 1).$$

This Lagrangian needs to be minimized with respect to  $\mathbf{w}$  and  $b$  and maximized with respect to  $\alpha_i$ —these are the Karush-Kuhn-Tucker conditions, described in optimization textbooks (e.g., see (Gill, Murray & Wright 1981)). A little manipulation leads to the requirements that

$$\sum_1^N \alpha_i y_i = 0$$

and

$$\mathbf{w} = \sum_1^N \alpha_i y_i \mathbf{x}_i.$$

This second expression is why the device is known as a *support vector machine*. Generally, the hyperplane is determined by a relatively small number of example points, and the position of other examples is irrelevant (see Figure 22.19; everything inside the convex hull of each set of examples is irrelevant to choosing the hyperplane, and most of the hull vertices are, too). This means that we expect that most  $\alpha_i$  are zero, and the data points corresponding to nonzero  $\alpha_i$ , which are the ones that determine the hyperplane, are known as the *support vectors*.

Now by substituting these expressions into the original problem and manipulating, we obtain the *dual problem* given by

$$\text{maximize } \sum_i^N \alpha_i - \frac{1}{2} \sum_{i,j=1}^N \alpha_i (y_i y_j \mathbf{x}_i \cdot \mathbf{x}_j) \alpha_j$$

$$\text{subject to } \alpha_i \geq 0$$

$$\text{and } \sum_{i=1}^N \alpha_i y_i = 0$$



You should notice that the criterion is a quadratic form in the Lagrange multipliers. This problem is a standard numerical problem known as *quadratic programming*. One can use standard packages quite successfully for this problem, but it does have special features—while there may be a large number of variables, most are zero at a solution point—which can be exploited (Smola et al. 2000).

**Algorithm 22.8:** Finding an SVM for a Linearly Separable Problem

**Notation:** We have a training set of  $N$  examples  $\{(\mathbf{x}_1, y_1), \dots, (\mathbf{x}_N, y_N)\}$  where  $y_i$  is either 1 or  $-1$ .

**Solving for the SVM:** Set up and solve the dual optimization problem:

$$\text{maximize } \sum_i^N \alpha_i - \frac{1}{2} \sum_{i,j=1}^N \alpha_i (y_i y_j \mathbf{x}_i \cdot \mathbf{x}_j) \alpha_j$$

subject to  $\alpha_i \geq 0$

$$\text{and } \sum_{i=1}^N \alpha_i y_i = 0.$$

Now  $\mathbf{w} = \sum_1^N \alpha_i y_i \mathbf{x}_i$  and for any example point  $\mathbf{x}_i$  where  $\alpha_i$  is nonzero, we have that  $y_i(\mathbf{w} \cdot \mathbf{x}_i + b) = 1$ , which yields the value of  $b$ .

**Classifying a point:** Any new data point is classified by

$$\begin{aligned} f(\mathbf{x}) &= \text{sign}(\mathbf{w} \cdot \mathbf{x} + b) \\ &= \text{sign}\left(\left(\sum_1^N \alpha_i y_i \mathbf{x} \cdot \mathbf{x}_i\right) + b\right) \\ &= \text{sign}\left(\sum_1^N (\alpha_i y_i \mathbf{x} \cdot \mathbf{x}_i + b)\right). \end{aligned}$$

### 22.5.2 Finding Pedestrians Using Support Vector Machines

At a fairly coarse scale, pedestrians have a characteristic, lollipoplike appearance—a wide torso on narrower legs. This suggests that they can be found using a support vector machine. The general strategy is the same as for the face-finding example in Section 22.4.4: Each image window of a fixed size is presented to a classifier, which determines whether the window contains a pedestrian. The number of pixels in the window may be large, and we know that many pixels may be irrelevant. In the case of faces, we could deal with this by cropping the image to an oval shape that would contain the face. This is harder to do with pedestrians because their outline is of a rather variable shape.

We need to identify features that can help determine whether a window contains a pedestrian. It is natural to try to obtain a set of features from a set of examples. A variety of feature selection algorithms might be appropriate here (all of them are variants of search). Oren, Pappageorgiou, Sinha, Osuna & Poggio (1997) chose to look at local features—*wavelet coefficients*,

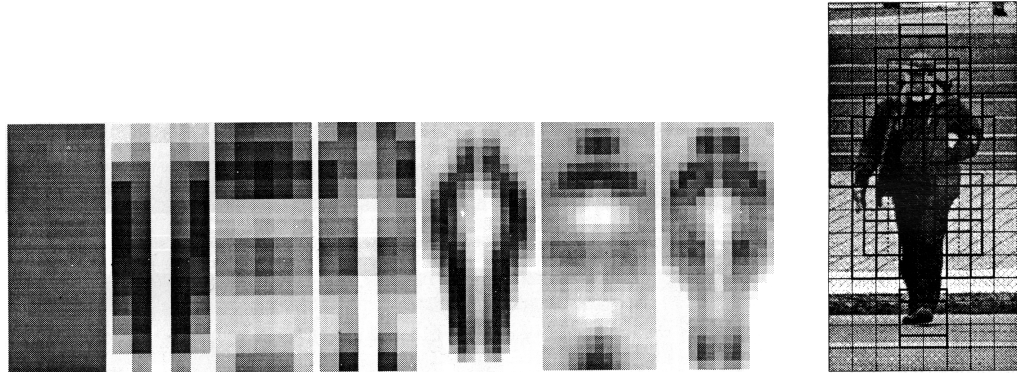


**Figure 22.20** On the **left**, averages over the training set of different wavelet coefficients at different positions in the image. Coefficients that are above the (spatial) average value are shown dark, and those that are below are shown light. We expect that noise has the average value, meaning that coefficients that are very light or very dark contain information that could identify pedestrians. On the **right**, a grid showing the support domain for the features computed. Notice that this follows the boundary of the pedestrian fairly closely. *Reprinted from, “A general framework for object detection,” by C. Papageorgiou, M. Oren and T. Poggio, Proc. Int. Conf. Computer Vision, 1998, © 1998, IEEE*

which are the response of specially selected filters with local support—and to use an averaging approach. In particular, they argued that the background in a picture of a pedestrian looks like noise, images that don't contain pedestrians look like noise, and the average noise response of their filters is known. This means that attractive features are ones whose average over many images of pedestrians is different from their noise response. If we average the response of a particular filter in a particular position over a large number of images, and the average is similar to a noise response, that filter in that position is not particularly informative (Figure 22.20).

Now that features have been chosen, training follows the lines of Section 22.5. The approach is effective (Figures 22.21 and 22.22). Bootstrapping (Section 22.4) appears to improve performance significantly.

## 22.6 NOTES

What classifier to use where is a topic one on which no orthodoxy is yet established. Instead, one tries to use methods that seem likely to work on the problem in hand. For the sake of brevity, we have omitted a vast number of useful techniques; there are several very useful books covering this area (Bishop 1995; Hastie, Tibshirani & Friedman 2001; Haykin 1999; McLachlan & Krishnan 1996; Ripley 1996; Vapnik 1996 and 1998 are good places to start).

Choosing a decision boundary is strictly easier than fitting a posterior model. However, with a decision boundary, there is no reliable indication of the extent to which an example belongs to one or another class, as there is with a posterior model. Furthermore, fitting a decision boundary requires that we know the classes to which the example objects should be allocated. It is by no means obvious that one can construct an unambiguous class hierarchy for the objects we encounter in recognition problems. Both approaches can require large numbers of examples to build useful classifiers. Typically, the stronger the model applied, the fewer examples required to build a classifier.



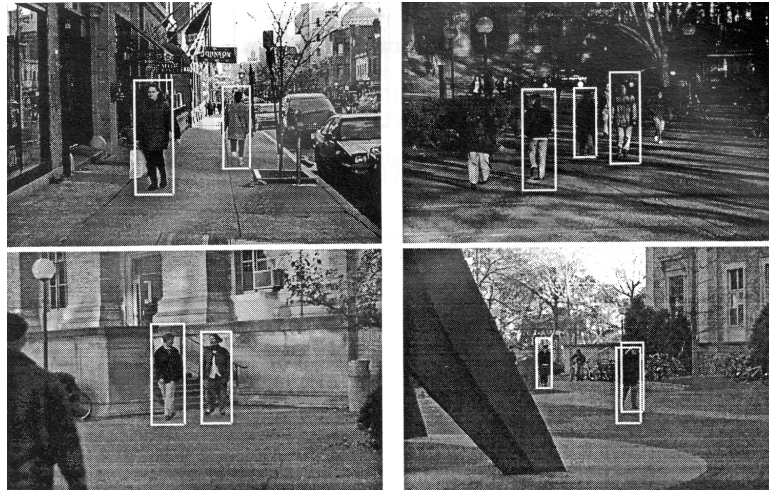


**Figure 22.21** Examples of pedestrians detected using the method of Papageorgiou, Oren, and Poggio. While not all pedestrians are found, there is a fairly high detection rate. The ROC is in Figure 22.22. Reprinted from, "A general framework for object detection," by C. Papageorgiou, M. Oren and T. Poggio, *Proc. Int. Conf. Computer Vision, 1998*, © 1998, IEEE

It is difficult to build classifiers that are really successful when objects have a large number of degrees of freedom without a detailed model of this variation, and classifiers tend to be difficult to use if the number of features can vary from example to example. In both cases, some form of structural model appears to be necessary. However, estimating, representing, and manipulating probability densities in the high-dimensional spaces that occur in vision problems is practically impossible unless very strong assumptions are applied. Furthermore, it is easy to build probability

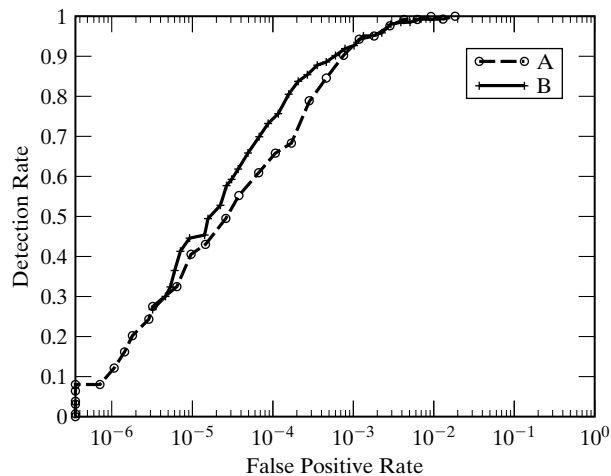


**Figure 22.22** The receiver operating curve for the pedestrian detection system of Papageorgiou, Oren, and Poggio. Reprinted from, "A general framework for object detection," by C. Papageorgiou, M. Oren and T. Poggio, *Proc. Int. Conf. Computer Vision, 1998*, © 1998, IEEE

models for which inference is again practically impossible. It isn't yet known how to build models that are easy to handle of the scale required for vision problems.

This subject is currently at the cutting edge of research in vision and learning. It's hard to know how to choose a method for a given problem, and opportunism seems to be the best approach at present. The examples in this chapter and the next illustrate a range of approaches that have been taken—some are very successful—but don't yet represent a clear theory.

An alternative approach to training one grand classifier is to train multiple classifiers and combine their outputs. This strategy is usually known as *boosting*. Boosting is most useful for classifiers with quite simple decision boundaries; these are usually easy to train, but have quite poor performance. Typically, we train a classifier and then determine the examples in the training set that it gets wrong. These examples are then emphasized—either by weighting errors on them more heavily or inserting copies into the training set—and a new classifier is trained. We now find out what the new classifier gets wrong and emphasize these examples and train again; this process continues through many iterations. Now the outputs of all the classifiers are combined using a set of weights.

### Skin Detection

There are a number of skin-detection papers; we selected one that fit with our didactic needs. Uses include finding naked people (Fleck, Forsyth & Bregler 1996, Forsyth & Fleck 1999) and finding and tracking faces and hands (Park, Seo, An & Chung 2000, Yoo & Oh 1999). There are a variety of techniques; for a start, look at the comparison of approaches in (Brand & Mason 2000). The performance of face finders seems to be improved by using skin detectors tuned one way or another; it seems natural to learn the skin detector at the same time as one learns the face finder, although we are not aware of work that does this.

### Face Finding

There is substantial interest in building face finders using template-matching techniques. The general strategy is to present image regions, possibly corrected for illumination variations, to classifiers of one form or another. We have taken liberties with history in our presentation; Schneiderman and Kanade's work appeared after Rowley, Baluja and Kanade's work which appeared at the same time as important work by Sung & Poggio (1998) We do not discuss this work for didactic reasons only. Osuna, Freund & Girosi (1997) produced a face finder that successfully used a support vector machine, and this class of method is now widely used.

Face recognition (whose face is this) is also important, and it isn't clear that recognition and finding should be divorced. Important papers include (Brunelli & Poggio 1993 and 1992). Significant technologies include recognition from very small numbers of examples (one would be great) (Beymer & Poggio 1995); recognition from different views (Beymer 1994); and managing variations induced by changes in illumination (Adini, Moses & Ullman 1997, Adini, Moses & Ullman 1994, Georghiades, Belhumeur & Kriegman 2000, Jacobs, Belhumeur & Basri 1998, Georghiades, Kriegman & Belhumeur 1998).

### Pedestrian Finding

The observation that pedestrians can be found using a template matcher is useful. As we have seen, the template looks rather like a lollipop. Although pedestrians may disappear if they raise their arms (because they no longer look like lollipops), they typically spend a fair amount of time with their arms at their sides, meaning that a reasonable count of the number of pedestrians

may be available. Furthermore, pedestrian movements are characteristic (Papageorgiou, Oren & Poggio 1998; Papageorgiou & Poggio 1999 and 2000).

## PROBLEMS

**22.1.** Assume that we are dealing with measurements  $\mathbf{x}$  in some feature space  $S$ . There is an open set  $D$  where any element is classified as class one, and any element in the interior of  $S - D$  is classified as class two.

(a) Show that

$$\begin{aligned} R(s) &= Pr \{1 \rightarrow 2 \mid \text{using } s\} L(1 \rightarrow 2) + Pr \{2 \rightarrow 1 \mid \text{using } s\} L(2 \rightarrow 1) \\ &= \int_D p(2 \mid \mathbf{x}) d\mathbf{x} L(1 \rightarrow 2) + \int_{S-D} p(1 \mid \mathbf{x}) d\mathbf{x} L(2 \rightarrow 1). \end{aligned}$$

(b) Why are we ignoring the boundary of  $D$  (which is the same as the boundary of  $S - D$ ) in computing the total risk?

**22.2.** In Section 22.2, we said that if each class-conditional density had the same covariance, the classifier of Algorithm 22.2 boiled down to comparing two expressions that are linear in  $\mathbf{x}$ .

(a) Show that this is true.

(b) Show that if there are only two classes, we need only test the sign of a linear expression in  $\mathbf{x}$ .

**22.3.** In Section 22.3.1, we set up a feature  $u$ , where the value of  $u$  on the  $i$ th data point is given by  $u_i = \mathbf{v} \cdot (\mathbf{x}_i - \boldsymbol{\mu})$ . Show that  $u$  has zero mean.

**22.4.** In Section 22.3.1, we set up a series of features  $u$ , where the value of  $u$  on the  $i$ th data point is given by  $u_i = \mathbf{v} \cdot (\mathbf{x}_i - \boldsymbol{\mu})$ . We then said that the  $\mathbf{v}$  would be eigenvectors of  $\Sigma$ , the covariance matrix of the data items. Show that the different features are independent using the fact that the eigenvectors of a symmetric matrix are orthogonal.

**22.5.** In Section 22.2.1, we said that the ROC was invariant to choice of prior. Prove this.

### Programming Assignments

**22.6.** Build a program that marks likely skin pixels on an image; you should compare at least two different kinds of classifier for this purpose. It is worth doing this carefully because many people have found skin filters useful.

**22.7.** Build one of the many face finders described in the text.

## 22.7 APPENDIX I: BACKPROPAGATION

The difficulty in training neural networks using stochastic gradient descent is that  $\nabla \text{Error}$  could be quite hard to compute. There is an effective strategy for computing  $\nabla \text{Error}$  called *backpropagation*. This approach exploits the layered structure of the neural network as a function of a function of a function, etc. to obtain the derivative.

Now recall the two layer neural net, which we wrote as

$$\mathbf{f}(\mathbf{x}) = [\phi(\mathbf{w}_{21} \cdot \mathbf{y}), \phi(\mathbf{w}_{22} \cdot \mathbf{y}), \dots, \phi(\mathbf{w}_{2n} \cdot \mathbf{y})],$$

where

$$\mathbf{y}(\mathbf{z}) = [\phi(\mathbf{w}_{11} \cdot \mathbf{z}), \phi(\mathbf{w}_{12} \cdot \mathbf{z}), \dots, \phi(\mathbf{w}_{1m} \cdot \mathbf{z}), 1]$$

and

$$\mathbf{z}(\mathbf{x}) = [x_1, x_2, \dots, x_p, 1].$$

We would like to compute

$$\frac{\partial Error}{\partial w_{kl,m}},$$

where  $w_{kl,m}$  is the  $m$ th component of  $\mathbf{w}_{kl}$ . Let us deal with the coefficients of the output layer first, so that we are interested in  $w_{2l,m}$  and get

$$\begin{aligned} \frac{\partial Error}{\partial w_{2l,m}} &= \sum_k \frac{\partial Error}{\partial f_k} \frac{\partial f_k}{\partial w_{2l,m}} \\ &= \frac{\partial Error}{\partial f_l} \frac{\partial f_l}{\partial w_{2l,m}} \\ &= \sum_e \left\{ (f_l(\mathbf{x}^e) - o_l^e) \frac{\partial f_l}{\partial w_{2l,m}} \right\} \\ &= \sum_e \left\{ (f_l(\mathbf{x}^e) - o_l^e) \phi'_{2l}(y_m(\mathbf{x}^e)) \right\} \\ &= \sum_e \left\{ \delta_{2l}^e(y_m(\mathbf{x}^e)) \right\}. \end{aligned}$$

Here, we use the notation

$$\phi'_{2l} = \frac{\partial \phi}{\partial u},$$

where the derivative is evaluated at  $u = \mathbf{w}_{2l} \cdot \mathbf{y}$ , and we write

$$\delta_{2l}^e = (f_l(\mathbf{x}^e) - o_l^e) \phi'_{2l}.$$

Notice that evaluating this derivative involves terms in the input of the layer—the terms  $y_m(\mathbf{x}^e)$ —and in its output—the terms  $\delta_{2l}^e$ .

Now consider the coefficients of the second layer. We are interested in  $w_{1l,m}$ , and we get

$$\begin{aligned} \frac{\partial Error}{\partial w_{1l,m}} &= \sum_k \left\{ \frac{\partial Error}{\partial f_k} \frac{\partial f_k}{\partial w_{1l,m}} \right\} = \sum_{i,j} \left\{ \frac{\partial Error}{\partial f_i} \frac{\partial f_i}{\partial y_j} \frac{\partial y_j}{\partial w_{1l,m}} \right\} \\ &= \left\{ \sum_k \frac{\partial Error}{\partial f_k} \frac{\partial f_k}{\partial y_l} \right\} \frac{\partial y_l}{\partial w_{1l,m}} \\ &= \sum_e \left\{ \sum_k \left\{ (f_k(\mathbf{x}^e) - o_k^e) \frac{\partial f_k}{\partial y_l} \right\} \frac{\partial y_l}{\partial w_{1l,m}} \right\} \\ &= \sum_e \left\{ \sum_k \left\{ (f_k(\mathbf{x}^e) - o_k^e) \phi'_{2k} w_{2k,l} \right\} \frac{\partial y_l}{\partial w_{1l,m}} \right\} \\ &= \sum_e \left\{ \sum_k \left\{ (f_k(\mathbf{x}^e) - o_k^e) \phi'_{2k} w_{2k,l} \right\} \phi'_{1l} z_m \right\} \\ &= \sum_e \left\{ \sum_k \left\{ \delta_{2k}^e w_{2k,l} \right\} \phi'_{1l} z_m \right\}. \end{aligned}$$

In this expression,

$$\phi'_{2k} = \frac{\partial \phi}{\partial u},$$

evaluated at  $u = \mathbf{w}_{2k} \cdot \mathbf{y}$ , and

$$\phi'_{1l} = \frac{\partial \phi}{\partial u},$$

evaluated at  $u = \mathbf{w}_{1l} \cdot \mathbf{z}$ . Now if we write

$$\delta_{1l}^e = \sum_k \{ \delta_{2k}^e w_{2k,l} \} \phi'_{1l},$$

we get

$$\frac{\partial E}{\partial w_{1l,m}} = \sum_e \delta_{1l}^e z_m(\mathbf{x}^e).$$

Again, this sum involves a term obtained computing the previous derivative, terms in the derivatives within the layer, and terms in the input. You should convince yourself that, if we had a third layer, the derivative of the error with respect to parameters within this third layer would have a similar form—a function of terms in the derivative of the second layer, terms in the derivatives within the third layer, and terms in the input (all this comes from aggressive application of the chain rule). This suggests a two-pass algorithm:

1. Evaluate the net's output on each example. This is usually referred to as a *forward pass*.
2. Evaluate the derivatives using the intermediate terms. This is usually referred to as a *backward pass*.

This process yields the derivatives of the total error with respect to the parameters. We can obtain another simplification: We adopted stochastic gradient descent to avoid having to sum the value of the error and of its gradient over all examples. Because computing a gradient is linear, to compute the gradient of the error on one example alone, we simply drop the sum at the front of our expressions for the gradient. The whole is given in Algorithm 22.7.

**Algorithm 22.9:** Backpropagation to compute the derivative of the fitting error of a two-layer neural net on a single example with respect to its parameters

**Notation:**

Write the two-layer neural net as

$$\begin{aligned} \mathbf{f}(\mathbf{x}; \mathbf{p}) &= [\phi(\mathbf{w}_{21} \cdot \mathbf{y}), \phi(\mathbf{w}_{22} \cdot \mathbf{y}), \dots, \phi(\mathbf{w}_{2n} \cdot \mathbf{y})] \\ \mathbf{y}(\mathbf{z}) &= [\phi(\mathbf{w}_{11} \cdot \mathbf{z}), \phi(\mathbf{w}_{12} \cdot \mathbf{z}), \dots, \phi(\mathbf{w}_{1m} \cdot \mathbf{z}), 1] \\ \mathbf{z}(\mathbf{x}) &= [x_1, x_2, \dots, x_p, 1] \end{aligned}$$

( $\mathbf{p}$  is a vector containing all parameters). Write the error on a single example as

$$\begin{aligned} \text{Error}^e &= \text{Error}(\mathbf{p}; \mathbf{x}^e) \\ &= \left(\frac{1}{2}\right) |\mathbf{f}(\mathbf{x}^e; \mathbf{p}) - \mathbf{o}^e|^2. \end{aligned}$$

We would like to compute

$$\frac{\partial Error^e}{\partial w_{kl,m}},$$

where  $w_{kl,m}$  is the  $m$ th component of  $w_{kl}$ .

**Forward pass:** Compute  $f(\mathbf{x}^e; \mathbf{p})$  saving all intermediate variables.

**Backward pass:** Compute

$$\begin{aligned}\delta_{2l}^e &= (f_l(\mathbf{x}^e) - o_l^e)\phi'_{2l} \\ \phi'_{2l} &= \frac{\partial \phi}{\partial u} \text{ evaluated at } u = \mathbf{w}_{21} \cdot \mathbf{y} \\ \frac{\partial Error^e}{\partial w_{2l,m}} &= \sum_e \{ \delta_{2l}^e (y_m(\mathbf{x}^e)) \}.\end{aligned}$$

Now compute

$$\begin{aligned}\delta_{1l}^e &= \sum_k \{ \delta_{2k}^e w_{2k,l} \} \phi'_{1l} \\ \phi'_{1l} &= \frac{\partial \phi}{\partial u} \text{ evaluated at } u = \mathbf{w}_{11} \cdot \mathbf{z} \\ \frac{\partial E^e}{\partial w_{1l,m}} &= \delta_{1l}^e z_m(\mathbf{x}^e).\end{aligned}$$

## 22.8 APPENDIX II: SUPPORT VECTOR MACHINES FOR DATASETS THAT ARE NOT LINEARLY SEPARABLE

In many cases, a separating hyperplane does not exist. To allow for this case, we introduce a set of *slack variables*,  $\xi_i \geq 0$ , which represent the amount by which the constraint is violated. We can now write our new constraints as

$$y_i (\mathbf{w} \cdot \mathbf{x}_i + b) \geq 1 - \xi_i,$$

and we modify the objective function to take account of the extent of the constraint violations to get the problem

$$\begin{aligned}\text{minimize } & \frac{1}{2} \mathbf{w} \cdot \mathbf{w} + C \sum_{i=1}^N \xi_i \\ \text{subject to } & y_i (\mathbf{w} \cdot \mathbf{x}_i + b) \geq 1 - \xi_i \\ & \text{and } \xi_i \geq 0.\end{aligned}$$

Here  $C$  gives the significance of the constraint violations with respect to the distance between the points and the hyperplane. The dual problem becomes

$$\begin{aligned} & \text{maximize } \sum_i^N \alpha_i - \frac{1}{2} \sum_{i,j=1}^N \alpha_i (y_i y_j \mathbf{x}_i \cdot \mathbf{x}_j) \alpha_j \\ & \text{subject to } C \geq \alpha_i \geq 0 \\ & \text{and } \sum_{i=1}^N \alpha_i y_i = 0. \end{aligned}$$

Again, we have

$$\mathbf{w} = \sum_i^N \alpha_i y_i \mathbf{x}_i,$$

but recovering  $b$  from the solution to the dual problem is slightly more interesting. For each example where  $C > \alpha_i > 0$  (note that these are strict inequalities, unlike the constraints), the slack variable  $\xi_i$  will be zero. This means that

$$\sum_{j=1}^N y_j \alpha_j \mathbf{x}_i \cdot \mathbf{x}_j + b = y_i$$

for these values of  $i$ . This expression yields  $b$ . Again, the optimization problem is a quadratic programming problem, although there is no guarantee that many points will have  $\alpha_i = 0$ .

## 22.9 APPENDIX III: USING SUPPORT VECTOR MACHINES WITH NON-LINEAR KERNELS

For many datasets, it is unlikely that a hyperplane will yield a good classifier. Instead, we want a decision boundary with a more complex geometry. One way to achieve this is to map the feature vector into some new space and look for a hyperplane in that new space. For example, if we had a plane dataset that we were convinced could be separated by plane conics, we might apply the map

$$(x, y) \rightarrow (x^2, xy, y^2, x, y)$$

to the dataset. A classifier boundary that is a hyperplane in this new feature space is a conic in the original feature space. In this form, this idea is not particularly useful because we might need to map the data into a high-dimensional space (e.g., assume that we know the classifier boundary has degree two, and the data is 10 dimensional—we would need to map the data into a 65 dimensional space).

Write the map as  $\mathbf{x}' = \phi(\mathbf{x})$ . Write out the optimization problem for the new points  $\mathbf{x}'_i$ ; you will notice that the only form in which  $\mathbf{x}'_i$  appears is in the terms

$$\mathbf{x}'_i \cdot \mathbf{x}'_j,$$

which we could write as  $\phi(\mathbf{x}_i) \cdot \phi(\mathbf{x}_j)$ . Apart from always being positive, this term doesn't give us much information about  $\phi$ . In particular, the map doesn't appear explicitly in the optimization problem. If we did solve the optimization problem, the final classifier would be

$$f(\mathbf{x}) = \text{sign} \left( \sum_i^N (\alpha_i y_i \mathbf{x}' \cdot \mathbf{x}'_i + b) \right) = \text{sign} \left( \sum_i^N (\alpha_i y_i \phi(\mathbf{x}) \cdot \phi(\mathbf{x}_i) + b) \right).$$



Assume that we have a function  $k(\mathbf{x}, \mathbf{y})$  that is positive for all pairs of  $\mathbf{x}, \mathbf{y}$ . It can be shown that, under various technical conditions of no interest to us, there is some  $\phi$  such that  $k(\mathbf{x}, \mathbf{y}) = \phi(\mathbf{x}) \cdot \phi(\mathbf{y})$ . All this allows us to adopt a clever trick—instead of constructing  $\phi$  explicitly, we obtain some appropriate  $k(\mathbf{x}, \mathbf{y})$  and use it in place of  $\phi$ . In particular, the dual optimization problem becomes

$$\begin{aligned} &\text{maximize } \sum_i^N \alpha_i - \frac{1}{2} \sum_{i,j=1}^N \alpha_i (y_i y_j k(\mathbf{x}_i, \mathbf{x}_j)) \alpha_j \\ &\text{subject to } \alpha_i \geq 0 \\ &\text{and } \sum_{i=1}^N \alpha_i y_i = 0, \end{aligned}$$

and the classifier becomes

$$f(\mathbf{x}) = \text{sign} \left( \sum_1^N (\alpha_i y_i k(\mathbf{x}, \mathbf{x}_i) + b) \right).$$

Of course, these equations assume that the dataset are separable in the new feature space represented by  $k$ . This may not be the case, in which case the problem becomes

$$\begin{aligned} &\text{maximize } \sum_i^N \alpha_i - \frac{1}{2} \sum_{i,j=1}^N \alpha_i (y_i y_j k(\mathbf{x}_i, \mathbf{x}_j)) \alpha_j \\ &\text{subject to } C \geq \alpha_i \geq 0 \\ &\text{and } \sum_{i=1}^N \alpha_i y_i = 0, \end{aligned}$$

and the classifier becomes

$$f(\mathbf{x}) = \text{sign} \left( \sum_1^N (\alpha_i y_i k(\mathbf{x}, \mathbf{x}_i) + b) \right).$$

There are a variety of possible choices for  $k(\mathbf{x}, \mathbf{y})$ . The main issue is that it must be positive for all values of  $\mathbf{x}$  and  $\mathbf{y}$ . Some typical choices are shown in Table 22.2. There doesn't appear to be any principled method for choosing between kernels; one tries different forms and uses the one that gives the best error rate measured using cross-validation.

TABLE 22.2 SOME SUPPORT VECTOR KERNELS

Kernel form	Qualitative properties of $\phi$ represented by this kernel
$(\mathbf{x} \cdot \mathbf{y})^d$	$\phi$ is all monomials of degree $d$
$(\mathbf{x} \cdot \mathbf{y} + c)^d$	$\phi$ is all monomials of degree $d$ or below
$\tanh(ax \cdot y + b)$	
$\exp\left(-\frac{(\mathbf{x}-\mathbf{y})^T(\mathbf{x}-\mathbf{y})}{2\sigma^2}\right)$	